Atmos. Chem. Phys. Discuss., 11, 28747–28796, 2011
www.atmos-chem-phys-discuss.net/11/28747/2011/
doi:10.5194/acpd-11-28747-2011

Atmospheric Chemistry and Physics Discussions

Ozonesonde climatology between 1995 and 2009: description, evaluation and applications

S. Tilmes[1], J.-F. Lamarque[1], L. K. Emmons[1], A. Conley[1], M. G. Schultz[2], M. Saunois[1,*], V. Thouret[3], A. M. Thompson[4], S. J. Oltmans[5], B. Johnson[5], and D. Tarasick[6]

[1]National Center for Atmospheric Research, Boulder, Colorado, USA
[2]Research Center Jülich, Jülich, Germany
[3]Laboratoire d'Aérologie, UMR 5560, Université Paul Sabatier, Toulouse, France
[4]NASA Goddard Space Flight Center, Greenbelt, Maryland, USA
[5]NOAA Climate Monitoring and Diagnostics Laboratory, Boulder, Colorado, USA
[6]Experimental Studies (ARQX), Air Quality Research Division, Environment Canada, 4905 Dufferin Street, Downsview, Ontario, Canada
[*]now at: Laboratoire des Sciences du Climat et de l'Environnement, CEA-CNRS-UVSQ, Gif-Sur-Yvette, France

Received: 1 October 2011 – Accepted: 11 October 2011 – Published: 26 October 2011

Correspondence to: S. Tilmes (tilmes@ucar.edu)

Published by Copernicus Publications on behalf of the European Geosciences Union.

Abstract

An ozone climatology based on ozone soundings for the last 15 years has been constructed for model evaluation and comparisons to other observations. Vertical ozone profiles for 41 stations around the globe have been compiled and averaged for the years 1980–1994 and 1995–2009. The climatology provides information about the median and the width of the ozone probability distribution function, as well as interannual variability of ozone between 1995 and 2009, in pressure and tropopause-referenced altitudes. In addition to single stations, regional aggregates are presented, combining stations with similar ozone characteristics. The Hellinger distance is introduced as a new diagnostic to compare the variability of ozone distributions within each region and used for model evaluation purposes. This measure compares not only the mean, but also the shape of distributions. The representativeness of regional aggregates is discussed using independent observations from surface stations and MOZAIC aircraft data. Ozone from all of these data sets show an excellent agreement within the range of the interannual variability, especially if a sufficient number of measurements are available, as is the case for West Europe. Within the climatology, a significant longitudinal variability of ozone in the troposphere and lower stratosphere in the northern mid- and high latitudes is found. The climatology is used to evaluate results from two model intercomparison activities, HTAP for the troposphere and CCMVal2 for the tropopause region and the stratosphere. HTAP ozone is in good agreement with observations in the troposphere within their range of uncertainty, but ozone peaks too early in the Northern Hemisphere spring. The strong gradients of ozone around the tropopause are less well captured by many models. Lower stratospheric ozone is overestimated for all regions by the multi-model mean of CCMVal2 models. Individual models also show major shortcomings in reproducing the shape of ozone probability distribution functions in various regions and different altitudes, which might have significant implications for the radiative budgets in those models.

ACPD

11, 28747–28796, 2011

1 Introduction

Ozone is one of the most important trace gases in the atmosphere, and is strongly influenced by changes in the environment due to anthropogenic activities, for example fossil fuel combustion and industrial processes (e.g., Lelieveld and Dentener, 2000), and biomass burning (e.g., Oltmans et al., 2010). In the troposphere, ozone is photochemically produced by the oxidation of volatile organic compounds (VOC) and carbon monoxide (CO) in the presence of nitrogen oxides (NO_x). Trends and variability of ozone in the troposphere are therefore strongly controlled by long-term changes in chemistry and transport, but are also affected by interannual variations of sporadically occurring pollution events, such as very intense forest fires, volcanic eruptions and stratospheric intrusions, resulting in regional differences in ozone. Tropospheric ozone at mid-latitudes is affected by the occurrence of stratosphere-troposphere exchange processes in connection to weather systems, which have a varying influence for different regions (Wernli and Sprenger, 2007; Sprenger et al., 2007; Tang and Prather, 2010; Kunz et al., 2011) and are impacted by gravity and Rossby wave signatures (Thompson et al., 2011b). Pollution outflow from large cities often results in enhanced surface ozone values, especially during summer months, reducing regional air quality downwind of cities and in remote areas. Most of these ozone sources are expected to increase with a warmer climate (Stevenson et al., 2006). Furthermore, changes in methane (CH_4) influence the global ozone background in the troposphere, but the magnitude of these changes is still poorly understood. (e.g., Crutzen, 1973; Vingarzan, 2004; Fiore et al., 2008).

In the upper troposphere and lower stratosphere (UTLS), ozone acts as an important greenhouse gas (Forster et al., 2007), and ozone in the stratosphere shields the Earth from harmful shortwave ultraviolet radiation. The most obvious impact of anthropogenic activities on stratospheric ozone is the occurrence of the ozone hole in the Antarctic stratosphere in the austral spring each year (WMO, 2007, 2010). The amount of ozone in the stratosphere is also controlled by the Brewer-Dobson circulation, which may be affected by climate change (Garcia and Randel, 2008). In addition, decreasing

ACPD
11, 28747–28796, 2011

temperatures in the upper stratosphere decrease the effectiveness of chemical ozone destruction in that region. On the other hand, decreasing temperatures in the Arctic polar stratosphere may increase the likelihood of severe chemical ozone depletion in spring (Rex et al., 2004). The overall effect of climate change on lower stratospheric ozone is not well understood (e.g., Eyring et al., 2010).

Comprehensive chemistry climate models are used to simulate past, present and future climate to understand the complex interplay between various processes in the troposphere (Gauss et al., 2006; Stevenson et al., 2006; Reichler and Kim, 2008), the UTLS and stratosphere (Eyring et al., 2010). A precise description of the geographical and vertical distribution of ozone and its seasonality for present day conditions is required to quantify the performance of the models and to eventually improve them (e.g., Lamarque et al., 2005; Fiore et al., 2008; Eyring et al., 2010). Available data sets for model evaluation include retrievals from satellite data, ozone column measurements from Dobson and Umkehr instruments, vertical profiles from ozone sondes, aircraft and lidar measurements, and a multitude of surface observations, often from regional air quality monitoring networks. To evaluate ozone in the stratosphere, a variety of satellite observations are available. While satellites in nadir-viewing geometry provide global coverage with good time resolution, they generally contain little information on the vertical distribution of ozone. Limb-sounder satellite observations have relatively high vertical resolution, but provide sparse global coverage and carry large uncertainties in the troposphere and the UTLS region. For the UTLS, in addition to satellite observations ozone soundings for the tropics and aircraft data for mid- and high latitudes are also used (Eyring et al., 2010). Surface measurements are of excellent quality and provide long-term records, but they can be influenced by local changes and pollution sources, which makes them less suitable for evaluation of coarse-scale models. Aircraft data from field campaigns are valuable for process understanding and have been used to derive climatologies (Tilmes et al., 2010), but they might not be representative for a larger region. Routinely-performed measurements from passenger aircraft are very well-suited to evaluate models in the troposphere and lowermost stratosphere

ACPD
11, 28747–28796, 2011

(Thouret et al., 1998a), but they are necessarily concentrated on major flight routes.

Here, we focus on data from ozonesondes, which provide some of the longest records over the entire globe and exhibit excellent vertical resolution from the surface up to 10 hPa. Logan (1999a,b) compiled global ozonesonde climatologies for the troposphere and stratosphere, respectively. An update was provided by McPeters et al. (2007) with focus on the stratosphere. Regional climatologies have been developed for the tropics (Thompson et al., 2003a; Thompson et al., 2011a,b; Randel and Thompson, 2011) and for the Southern Hemisphere subtropics (Clain et al., 2009). Individual ozone stations over different regions were compared to surface observations and analyzed for trends (Oltmans et al., 2006). However, to our knowledge, no updated global climatology for the last 15 years exists that focuses on the troposphere and the lower stratosphere. A new climatology including a more detailed description of the global ozone distribution and interannual variability is needed to provide a basis for present-day model evaluation.

The goal of this paper is to construct and discuss an ozone climatology for model evaluation with focus on the troposphere and lowermost stratosphere, based on available ozone soundings between 1995 and 2009. This climatology is provided to the community (Appendix A). A climatology between 1980 and 1994 is also provided, which is very similar to the climatology by Logan (1999a,b) (see Supplement). However, we do not discuss the climatology between 1980 and 1994 in detail, due to limited observations and some doubts about the quality of the earlier measurements (Smit et al., 1998). Besides single stations, we construct climatologies for various regions in combining stations with similar characteristics, as discussed in Sect. 2. The variability of ozone within the different regions is investigated in Sect. 3. We introduce a new diagnostic that provides a measure for the similarity of two ozone distributions by employing the Hellinger distance (Nikulin, 2001), defined in Appendix B. The Hellinger is applicable for comparisons of distributions of various shapes, including non-Gaussian distributions, as often observed in the atmosphere, for example in the UTLS region (Pan et al., 2010; Tilmes et al., 2010).

ACPD
11, 28747–28796, 2011

The representativeness of the ozone climatology for different regions is discussed in Sect. 4, using available hourly surface ozone data from the World Data Center for Greenhouse Gases (WDCGG) (http://gaw.kishou.go.jp/wdcgg/), the Clean Air Status and Trends Network (CASTNET) for the US (http://java.epa.gov/castnet/), the European Monitoring and Evaluation Programme (EMEP) network in Europe (http://www.emep.int/), and MOZAIC aircraft observations (http://mozaic.aero.obs-mip.fr/web) (Thouret et al., 1998b) for comparison.

We provide information about the time evolution of ozone (Sect. 5) and the number of observations per year and stations entering the climatology. In addition, we calculate decadal changes of ozone between 1990–1999 and 2000–2009 for different regions. Furthermore, we provide vertical ozone profiles in pressure altitudes and tropopause-referenced altitudes, averaged ozone profiles over 15 years for each season, as well as information about the interannual variability (defined here as the range of the 5th and 95th percentile of the annual median ozone value and the half-width of the distribution (defined here as the range of the 25th and 75th percentile) of ozone profiles (see Sect. 6). As an application, in Sect. 7, we compare this climatology to a range of tropospheric and stratospheric models that participated in two major international model intercomparison activities, HTAP and CCMVal. Summary and conclusions are provided in Sect. 8.

2 Selected Ozonesondes and Regions

Ozone soundings between 1980 and 2009 were compiled from the collection of the World Ozone and Ultraviolet data Center (WOUDC) (http://www.woudc.org/), from the NOAA Earth system Research Laboratory (ESRL), from the Global Monitoring Division (GMD, ftp://ftp.cmdl.noaa.gov/ozwv/ozone/) for Boulder and Hilo, and from the Southern Hemisphere ADditional OZonesondes (SHADOZ) between 1998–2009 (Thompson et al., 2003a,b). We consider 41 stations (shown in Fig. 1 and listed in Table 1) that have a sufficiently complete record of continuous sampling between 1995 and 2009

ACPD
11, 28747–28796, 2011

with at least 12 profiles per season for at least 5 continuous years (see supplemental material, Fig. S3, bottom plot of each panel).

For most of the stations, the Electrochemical Concentration Cell (ECC) ozone sonde was used. For Hohenpeissenberg and Payerne, Brewer-Mast ozone sondes were used, and for all Japanese stations, Kagoshima, Sapporo, Tateno, Naha, and Syowa, Carbon-Iodine Japanese Sondes (KC79/JMA) were used. Details about different ozone sonde types are given in Smit et al. (1998). As determined in the Jülich Ozone Sonde Intercomparison Experiment (JOSIE) (Smit et al., 1998), ozone sondes perform best in the lower stratosphere between the tropopause and 20 km altitudes, with a precision of about ±2–3 % for ECC-sondes, and a precision of ±5 % for Brewer-Mast and Carbon-Iodine sondes. In the troposphere, ECC-sondes show a precision of ±3–4 %, whereas the Brewer-Mast and Carbon-Iodine sondes exhibit a precision of of about ±4–8 %. In the troposphere, ECC-sondes show a small bias of ±3 %, the Brewer-Mast sondes show a negative bias of −3 %, and the Japanese sondes a negative bias between −2 and −7 %. The accuracy of the different sondes are about ±4–8 % for ECC-sondes and between 6 and 13 % for the Brewer-Mast and Japanese sondes.

Ozone profiles are employed, including already performed corrections of most of the stations by the data centers. In addition, we applied a column ozone filter to all ozone profiles to reject single profiles with column ozone values of more than 700 DU or of less than 50 DU. In this way, we also filter out unrealistic values of ozone profiles (in partial pressure) at the stratospheric maximum. For observations used here, ignoring profiles corrected by factors outside the range of 0.8 and 1.2 has only a small impact on the averaged profile between 1995 and 2009 (see Fig. S1).

The selected ozonesonde data in mixing ratios and partial pressure are averaged to 26 standard pressure levels between 1000 hPa and 1 hPa. Between 1000 hPa and 100 hPa, a layer thickness of 25 hPa centered on the selected pressure level was employed Between 100 hPa and 10 hPa a layer thickness of 2.5 hPa and above 10 hPa a layer thickness of 0.25 hPa was chosen. For the two NOAA stations employed (Boulder and Hilo), ozone profiles have been provided on a vertical grid of 250 m resolution. In

ACPD
11, 28747–28796, 2011

this case, ozone sonde data are linearly interpolated to the fixed pressure levels. Seasonal ozone profiles are derived by averaging available ozone observations between 1980 and 1994 and between 1995 and 2009 at all pressure levels (and tropopause-referenced altitude levels) for each station. The number of profiles entering each period is listed in Table 1. A comparison between the climatology for the period 1980 – 1994 and the climatology derived by Logan (1999a) for a similar period shows a good agreement between the two data sets (see supplemental material, Fig. S2).

Between 1995 and present, the number of available ozone soundings has greatly increased and a larger number of stations with records of several years has become available over the globe (Fig. S3). Years with a sampling-frequency of less than 12 profiles per season often deviate from other years and are therefore less reliable. For model evaluation purposes it is important to be aware of the number of profiles that entered the 15-yr averaged profiles and therefore the reliability of the values derived for single stations. This is particularly important for the earlier period of 1980-1994 when the number of soundings were often limited. Between 1995 and 2009, for most stations the entire period is covered about equally with sufficient ozone soundings per season, as discussed in the supplement. A comparison between 1980 – 1994 and 1995 – 2009 ozone profiles for each station is given in Fig. S4, Supplement).

The stations of regions with similar ozone characteristics are combined in order to obtain a sufficient sample size for tests of significance. Regional aggregates are better suited for model evaluation purposes, especially for models with a coarse horizontal resolution that would not capture small-scale variations in the ozone field (e.g., Emmons et al., 2010). The regions are (see Fig. 1, different colors): the western part of the Northern Hemisphere polar region (NH Polar West), the eastern part of the Northern Hemisphere polar region (NH Polar East), Canada, United States of America (US), West Europe, Japan, the Tropics, the Southern Hemisphere mid-latitudes (SH midlat), which only covers longitudes between 135°– 180°E, and the Southern Hemisphere polar region (SH Polar). The NH polar region is divided into an eastern and western sector, because of different tropospheric ozone characteristics, showing larger ozone

ACPD
11, 28747–28796, 2011

mixing ratios in the western sector in spring and summer, as further discussed in the supplemental material (Fig. S5, supplemental material). Besides the Tropics, we also consider the NH Sub-tropics (representing a region between 15–30°N).

All tropical stations are combined into only one region. The characteristics of tropospheric ozone over tropical stations differ depending on various processes: the location of the station with regard to the ascending or descending branch of the Walker circulations, the seasonality of convection, the influence of biomass burning, the amount of pollution and stratospheric influence (Thompson et al., 2011b). Further, gravity wave activity is most prevalent over the Pacific and Indian Oceans. The vertical structure of ozone and the interannual variations of a 10-yr period are distinct from station to station (Thompson et al., 2011b). A grouping of the tropical region into sub-regions is therefore difficult and would include at most two stations per region. Therefore, we provide information for one region only, to characterize ozone in the Tropics in contrast to higher latitudes. For detailed model evaluation of tropospheric ozone in the tropical region a comparison of single stations is likely to be more meaningful. Above the tropopause, tropical ozone mixing ratios of different stations are more similar, as discussed below.

3 Variability of ozone within different regions

We investigate the variability of ozone distributions within each region, in calculating the Hellinger distance and the relative difference of medians between different stations and the regionally-aggregated distribution, as introduced in Appendix B. The Hellinger distance is a measure of differences in the shape of distributions, not necessarily Gaussian. This measure scales between 0 and 1, whereby small values (below 0.1) occur for very similar distributions and 1 for completely different distributions. We derive the ozone probability distribution function (PDF) and the corresponding cumulative distribution functions (CDF) using all observations taken during a 15-yr period between 1995 and 2009. To calculate the Hellinger distance, the CDF is derived based on 25 variable bin sizes (see Appendix B for more details). Profiles are considered within

ACPD
11, 28747–28796, 2011

three altitude intervals above and below the thermal tropopause. Temperature information from ozone soundings is used to derive the thermal tropopause (TP), based on the temperature lapse rate definition (World Meteorological Organization, 1957).

The shape of ozone distributions in the UTLS depends on the altitude interval (with regard to the thermal tropopause), season and region (see Fig. 2, top and middle panel). For West Europe, most stations have similar ozone distributions for all seasons in the UTLS. Consequently, the Hellinger distances are less than 0.1 and the median differences are within ±10 %, for the majority of stations (different colors). The Hellinger distance exposes differences not only in the mean but also in the shape as can be seen in the case of Madrid in summer and fall in 1–3 km above the TP (see Fig. 2, bottom middle panel, pink symbols).

For the high northern latitudes and Canada, ozone distributions of all stations within each region are also very similar (see Fig. 3, top row). Most stations within one region show a median difference of less than ±10 % in comparison to the regional median and a Hellinger distance of around 0.1. A larger spread of the median difference and the Hellinger distance occurs for the US and Japan (Fig. 3, middle row). For the US, Japan (see also Appendix B) and the SH mid latitudes, a large variability of ozone distributions occurs in lowermost stratosphere during winter and spring. For the Tropics, a large variability of ozone can be identified in the troposphere, as discussed above. On the other hand, tropical ozone distributions in the lower stratosphere are rather similar and have a Hellinger distance of less than 0.1 from the regionally-aggregated distribution and a median difference within ≈ ±20 %. In the SH Polar region within ±3 km around the TP, ozone mixing ratios from different stations show a very similar distribution, with a Hellinger distance below 0.1 and a median difference of less than ±10 %.

The Hellinger distance between different observations as well as the variation in median of ozone distributions within each region provides a baseline for understanding the comparisons of models with observations.

ACPD
11, 28747–28796, 2011

4 Representativeness of regional averages in comparison to independent observations

The compilation of ozone profiles for different regions, based on a different number of stations considered depending on the region, raises the question about the representativeness of ozone averages for different regions. Here, we use independent data from surface ozone measurements and routinely performed passenger aircraft samples from the MOZAIC program (http://mozaic.aero.obs-mip.fr/web) (Thouret et al., 1998b) to compare regional and seasonal aggregates of ozone measurements derived from soundings between 1995 and 2009 (see Fig. 4, left panels, and Fig. 5, left and middle panels). Vertical profiles from MOZAIC are available at three locations in the eastern part of the US and for two airports in Japan. We also compare ozone sonde data that were taken in the area of Frankfurt in Europe to MOZAIC data taken in Frankfurt.

In addition, hourly surface observations from the EMEP network are available for over 60 stations in western Europe in the area around Germany and up to 17 stations for the eastern NH Polar region from EMEP and WDCGG database. Further, three surface stations in SH mid-latitudes and four in high latitudes in the SH are available from the WDCGG network (as shown in Fig. 4, right column, red diamonds). A large number of surface stations (about 120 stations) are also available for the US from the CASTNET network with up to 26 stations in southeast US. Only two surface stations are available for Japan, using WDCGG data (Fig. 5, bottom right panel). Altitude information of surface stations is included in Fig. 4 (right panels, different sizes of diamonds, going from small to large with increasing altitude). For Japan and high latitudes, surface data are only available in altitudes below 500 m.

Surface stations located at higher elevations have been shown to observe airmasses from higher altitudes than lower stations (e.g, Fiore et al., 2008). To compare similar airmasses between ozone sounding and surface measurements, we average surface ozone measurements that were taken within three altitude intervals, 0–500 m, 500–1500 m and >1500 m within each region. These are compared to all

ACPD
11, 28747–28796, 2011

available ozonesonde observations, interpolated to three corresponding pressure intervals (1000 hPa ± 50 hPa, 900 hPa ± 50 hPa and 800 hPa ± 50 Pa) and averaged for each region between 1995 and 2009. Aircraft observations and ozone soundings are compared for three pressure level intervals, 800 hPa ± 50 hPa, 500 hPa ± 50 hPa and 400 hPa ± 50 hPa. Timelines of the measurements for NH Polar, West Europe are given in Figs. S5 and S6, respectively.

The correlation between ozone soundings and surface ozone observations are shown in Figs. 4 and 5 (left column). The correlation between ozone soundings and MOZAIC data are shown in Fig. 5 (middle column). In general, ozonesonde data and surface ozone observations show reasonable agreement for all seasons and altitude levels, with correlation coefficients larger than 0.8 for all regions except Japan. For the eastern NH polar region, ozone soundings are biased high at the 1000 hPa level, which is likely due to the different regional coverage of those data. The largest deviations, up to 10 ppb, occur in fall. For the SH mid- and high latitudes, surface ozone data tend to be up to 8 ppb larger than those from ozonesondes. Besides the low bias of ozone soundings, the different data sets in the SH Polar region are also highly correlated. As for the high northern latitudes, only a limited amount of data around 1000 hPa is available in the SH. The variability of surface ozone distributions for different stations in the SH mid- and high latitudes is relatively large – resulting in a Hellinger distance of up to 0.3 – which can lead to discrepancies as a result of different regional coverage. The Hellinger distance between surface observations and ozone soundings is between 0.1 and 0.3 for these three regions, which is within the range of the variability of ozone soundings in each region.

For West Europe, we find a remarkable agreement between ozonesonde observations and surface measurements within ±4 ppbv, for all pressure levels and seasons, and a correlation coefficient of 0.97 (Fig. 5, first row). The Hellinger distance between surface data and soundings is below 0.2 in the lower troposphere, and within the range of the variability of single ozone stations to the regionally-aggregated mean. The very good agreement between the two data sets is related to the fact that for both surface

ACPD
11, 28747–28796, 2011

data and sondes, sufficient observations are available for all the pressure intervals considered. Furthermore, ozone sondes also show an excellent agreement with MOZAIC data over Frankfurt in the lower troposphere. MOZAIC observations are slightly smaller in the free troposphere compared to ozone soundings, but the data sets still agree within the error bars.

For the US, only three ozonesonde stations with long-term measurement records are available. Two of those are located in the southeast US, whereas the other, Boulder, CO, is close to the Rocky Mountains. Since surface ozone observations are variable across the US (e.g., Reidmiller et al., 2009) and soundings are not distributed over the entire region, we perform two comparisons, first for the southeast US, using data from two ozonesonde stations and surface observations within the black box in Fig. 5, top row, and second for the entire US, using the three soundings and all the surface observations. The comparison for southeast US shows a reasonable agreement with slightly larger ozone from soundings, especially in summer. For the entire US, ozone soundings are higher by up to 20 ppb compared to surface measurements, especially in summer. The shape of the ozone distributions from soundings is very different compared to surface observations, reaching a Hellinger distance of above 0.4, which is much larger than the variability of the ozone soundings in the US. For the most part, the ozone distribution from surface stations is shifted to lower values compared to the soundings (not shown). However, considering the under representation of ozonesondes compared to surface measurements, and the variability of ozone over the US (e.g., Reidmiller et al., 2009), a correlation coefficient of 0.86 is rather good. On the other hand, ozonesondes and MOZAIC aircraft data for altitudes between 800 hPa and 400 hPa agree within the variability of both observations for southeast US and the entire US, except for summer.

The relatively few surface ozone data and ozone soundings in Japan agree within 8 ppbv, which is within the interannual variability. Comparisons of MOZAIC aircraft and surface data in China have demonstrated a large daily variability of ozone at the surface (Ding et al., 2008) that might have a significant impact on ozone over Japan. Indeed, ozone sonde observations show a large variability among the stations, however,

ACPD
11, 28747–28796, 2011

the regional aggregates agree well with surface observations. The comparison with MOZAIC data shows a good agreement. The correlation between ozone soundings and independent observations is smaller ($r = 0.64$), however this is likely a result of a larger interannual variability.

In summary, one has to be careful in comparing regional averages of model results to regionally-aggregated distributions from observations for under-represented regions, which can result in misleading results. This is especially true for regions that show a large regional variability, as is the case for surface values in the US and regions in the SH. For model evaluation, we therefore recommend performing regionally-aggregated comparisons between observations and model results, as we do in Sect. 7.

5 Time evolution for different seasons and pressure levels

Timelines of ozone vary depending on region, season and altitude levels, as illustrated in Figs. 6 and 7. To illustrate the interannual variability independent of the seasonal variability, we consider seasonal and regional aggregates of ozone for the troposphere and stratosphere, respectively, showing the median of the distribution and the half-width of the distribution as error bars.

Ozone in the troposphere and stratosphere is influenced by a variety of dynamical processes, including ENSO, Rossby waves, and gravity waves, as shown for the tropics (e.g., Randel and Thompson, 2011; Thompson et al., 2011b). The interannual variability of stratospheric ozone has been shown to impact the interannual variability of tropospheric ozone (Tarasick et al., 2005; Hess and Zbinden, 2011). Volcanic eruptions also have a significant impact, especially on stratospheric ozone. In the troposphere, ozone is further affected by anthropogenic activities and significant pollution events like the very large forest fires in 2003 (connected to ENSO). The importance of different components that influence the interannual variability of ozone in different parts of the atmosphere, especially for the troposphere, has to be investigated in more detail and cannot be directly revealed from the ozone timelines, shown in Fig. 6. For

ACPD
11, 28747–28796, 2011

model evaluation purposes, we define the interannual variability as the range of the 5th and 95th percentile of the annual averaged ozone (calculated as: (95th percentile – 5th percentile)/2.). This measure will allow a general comparison of interannual variability between models and observations in different regions. The interannual variability and the half-width of the 15-yr average are quantified and discussed in Sect. 6

In general, ozone mixing ratios in the troposphere in spring (not shown) and summer show the largest values and the largest variability between the years. This is consistent with earlier findings (e.g., Logan, 1999a). Typically, tropospheric timelines show significant differences between different regions, suggesting longitudinal variations in mid and high latitudes in the NH. On the other hand, the interannual variability within a region and season is often very similar for different pressure levels (as further discussed in Sect. 6).

In the stratosphere (Fig. 7), in high northern latitudes, maximum mixing ratios occur in winter (and spring, not shown) at 100 hPa and 50 hPa, as a result of enhanced ozone transport due to the Brewer-Dobson circulation. The increase of ozone between summer and winter is most marked below 10 hPa. In contrast, over the high southern latitudes, the smallest ozone mixing ratios occur in SH austral winter and spring, as the result of the occurrence of the ozone hole. Spring and summer values are larger compared to their counterpart in the polar NH. Mid-latitude ozone is, in general, larger than in the high latitudes above the 50 hPa pressure level. Significant differences between different regions are also observed in the stratosphere. For example, ozone in western Europe is more similar to the characteristic of the high northern latitudes, while the US and Japan are more similar to the values in the Tropics, as further discussed below.

Based on median ozone mixing ratios for each season and pressure level, we quantify the changes of ozone between the periods 1990–1999 and 2000–2009. We only consider those regions where at least 8 years of measurements are available in each period (see Fig. 8). We note that in general ozone trends have been shown to be small if significant for the last 15 years (Oltmans et al., 2006). Significant changes of ozone based on the Student's t test between 1990–1999 and 2000–2009 (shown as large plus

ACPD
11, 28747–28796, 2011

signs in Fig. 8) occur for the most part in the troposphere and the mid-stratosphere. In general, changes of ozone between 1990–1999 and 2000–2009 vary with altitude and season. For the NH polar region and Canada, ozone mixing ratios have increased by 5–10 % within the last 20 years, most significantly in winter and spring. On the other hand, ozone has decreased by 3–8 % over West Europe in the upper troposphere and over Japan in the lower troposphere for winter and spring. In the UTLS, ozone in the NH Polar West region shows a decline in fall, similar to West Europe, whereas ozone has increased in spring in NH Polar East, Canada, West Europe and Japan, although the changes are mostly not significant. In the stratosphere, significant changes are only found in the NH Polar West region in summer and fall, with an increase of 10–15 % between 1990–1999 and 2000–2009 and in winter in the NH Polar East region. The increase of ozone in high northern latitudes is likely related to changes in the Brewer-Dobson circulation (Bönisch et al., 2011). Strongly decreasing ozone mixing ratios between 1990–1999 and 2000–2009 occur in the lower stratosphere of the SH Polar region in austral spring of more than 50 %. Minimum ozone values have strongly decreased in the early nineties as the result of increasing ozone depletion due to halogen chemistry. Between 2000 and 2009, some years experienced enhanced ozone values in the lower stratosphere (for example 2002 and 2004, as a result of a larger dynamical activity in those years), but no significant trend has been observed during the last 10 years (not shown).

6 Vertical profiles for different seasons and regions

For model and data comparisons, we provide regionally and seasonally aggregated ozone profiles for 1995 – 2009 in pressure altitudes and tropopause-referenced altitudes, as discussed in the following (see Fig. 9). In high northern latitudes, surface ozone mixing ratios in summer are lowest compared to the other seasons. The similarity of tropospheric ozone over the western sector of the NH polar region to West Europe suggests the influence of European airmasses. Further, the eastern sector

ACPD
11, 28747–28796, 2011

is more similar to ozone over Canada. Ozone profiles over the US and Japan show more tropical characteristics and a higher ozonopause (defined as the altitude with the strongest ozone gradient) in summer and fall compared to West Europe. A seasonality of the height of the ozonopause is also obvious in the Tropics, with a maximum in DJF and MAM. A secondary ozone minimum in the upper troposphere is especially obvious in winter for the NH Sub-tropics and in spring (MAM) for the Tropics (Logan, 1999a). Structure and zonal variability of UT ozone in the tropics are described in Thompson et al. (2011b,a) and so are not shown here. A lower mixing ratio is characteristic in the UT over the western Pacific (Samoa, Watukosek, Fiji) than over the Atlantic (Natal, Ascension), with the equatorial Americas (San Cristobal and Paramaribo (Thompson et al., 2010)), representing a transition region between the two. Tropospheric ozone in the SH mid-latitudes shows a different seasonality than in the NH. Largest ozone mixing ratios occur in the SH winter and spring and smallest in summer and fall.

To investigate processes in the UTLS, we consider ozone in tropopause-referenced altitudes. The seasonality of ozone in the UTLS is mostly a result of the influence of transport processes on ozone (e.g., Thouret et al., 2006). The Brewer-Dobson circulation transports high ozone mixing ratios towards mid- and high latitudes most pronounced in winter and spring. On the other hand, isentropic exchange between the tropics and extra-tropics is important (Bönisch et al., 2009; Birner and Bönisch, 2011; Tilmes et al., 2010) and influences ozone in the lowermost stratosphere. The seasonality of tropopause-referenced altitudes (Fig. 10) can be very different from the seasonality of ozone at pressure altitudes, as also noted in Eyring et al. (2010). For example, in Japan at the 200 hPa level (Fig. 9), ozone is lowest in summer and fall and largest in winter and spring as a result of a higher TP in summer and fall compared to winter and spring. Considering TP-referenced altitudes within 2 km above the TP (Fig. 10), lowest ozone mixing ratios occur in winter, and largest in summer. The seasonality in the lowermost stratosphere can therefore strongly depend on the coordinate system considered. Over high northern latitudes and in West Europe and Canada, ozone mixing ratios in the lowermost stratosphere are smaller in fall and winter than in spring

ACPD
11, 28747–28796, 2011

and summer, in agreement with findings from Thouret et al. (2006) based on MOZAIC aircraft observations. However, the seasonality over the US and Japan is different; the lowest ozone mixing ratios occur in winter and spring. This might be linked to the larger frequency of stratospheric tropospheric exchange processes in these regions, as found by (Wernli and Sprenger, 2007; Sprenger et al., 2007). It is therefore important to consider different regions in the NH mid-latitudes to capture the longitudinal gradient in the lowermost stratosphere.

The seasonality of ozone for the NH Tropics above the tropical TP, showing smallest ozone mixing ratios in winter and largest in summer, is in agreement with earlier studies (Folkins et al., 2006; Randel et al., 2008; Tilmes et al., 2010). Evidence for tropical and subtropical TP trends in the SH is presented by Sivakumar et al. (2011). For the SH mid-latitudes the seasonality of ozone in the lower stratosphere is similar to NH mid-latitudes in West Europe. However, ozone mixing ratios are slightly lower for all seasons, likely because of the weaker Brewer-Dobson circulation in the SH compared to the NH. The lowermost stratosphere over the SH polar region is strongly influenced by the occurrence of the Antarctic ozone hole, resulting in very low ozone mixing ratios in SH spring.

Besides the median of the vertical profiles, we describe the variability of the distribution at different pressure and tropopause-referenced altitude levels. Since ozone distributions are for the most part not Gaussian (as discussed above), we are not considering the standard deviation, but quantifying the half-width of the distributions at each pressure level, as defined above. For model evaluation, we provide information about the interannual variability of ozone mixing ratios including trends for different stations and regions (Figs. 9 and 10 middle and right plot of each panel).

The width of the ozone probability density distribution is in general increasing with altitude, e.g., larger variability occurs at 400 hPa (200 hPa for the Tropics), due to an increasing impact of stratospheric air with increasing altitude and strong variability caused by transport (Lefohn et al., 2001). Maximum values of the width of the distribution (up to 50 %) occur around the TP. The interannual variability for the last 15 years

ACPD
11, 28747–28796, 2011

and the width of the distribution are in general similar for all pressure levels in the troposphere, which suggests that ozone is often influenced by the same factors within each region and season throughout the troposphere.

Considering the ozone distribution with regard to tropopause-referenced altitudes, the width of the distribution and the interannual variability around and above the TP are much smaller (around 20 %), which indicates that the variability of the TP height within each season is a significant factor for the large variability in ozone in the lowermost stratosphere if considering pressure levels (e.g. Pan et al., 2004). For the US and Japan, the half-width of the distribution and the interannual variability still reach 20–30 % of the median ozone values, even if considering tropopause-referenced altitudes. This indicates a strong variability in the influence of exchange processes between tropical and extra-tropical airmasses. In the Tropics the half-width of the distribution above the TP is larger in tropopause-referenced altitudes than considering pressure altitudes, in agreement with earlier studies (Thompson et al., 2011b,a; Randel and Thompson, 2011). For the SH mid-latitudes the interannual variability in the troposphere in spring and summer is larger than the half-width of the distribution. The largest variability and interannual variability of the ozone distribution occurs in spring in high southern latitudes during the ozone hole season.

7 Application of the ozone climatology to model studies

The new climatology (between 1995 and 2009) is used to evaluate simulated ozone concentrations from a set of models taking part in two modeling comparison efforts: HTAP for the troposphere and CCMVal2 for the UTLS and stratosphere. Model results are interpolated to all ozonesonde stations considered before they are regionally-aggregated for the comparison between model results and observations (as suggested above).

For the evaluation of chemistry and transport in the troposphere, and particularly to advance the understanding of hemispheric transport of air pollutants in the

ACPD
11, 28747–28796, 2011

Northern Hemisphere, the Task Force on Hemispheric Transport of Air Pollution (HTAP; www.htap.org) was established under the United Nations Economic Commission for Europe (UNECE) Convention on Long Range Transboundary Air Pollution (CLRTAP) (Keating and Zuber, 2007). In HTAP, 22 models participated that ran year 2001 with different meteorological fields and individual emissions, although a standard emission data set was provided which many models used (see Fiore et al. (2008) for details). The year 2001 was simulated and output was stored as monthly mean values. Since the modeling effort focused on processes in the NH, we only compare the NH high latitudes and the NH mid-latitudes. We compare the seasonal cycle of available model results for the year 2001 to measurements (Fig. 11, first to third row), as well as vertical profiles in pressure coordinates (fourth and fifth row).

The majority of the HTAP models show a reasonable ozone seasonality compared to observations (not shown). The correlation coefficient for the multi-model mean is 0.88 – 0.98 at the 800 hPa level in high northern latitudes, West Europe and the US, and 0.72 for Japan. The seasonality is less well reproduced in the upper troposphere, with a too early peak for all the regions. The mean bias between models and observations is largest at 200 hPa for high northern latitudes, where models show a large variability (not shown). Most models strongly underestimate ozone over high northern latitudes (mean bias of 142 ppb) and West Europe in spring. These discrepancies are also visible in ozone profiles Fig. 11 (fourth and fifth row). Models fail to capture the steep ozone gradients across the TP, which results in an overestimation of ozone in the upper troposphere around 400 hPa, especially in winter. Further, simulated ozone profiles point to differences in the height of the TP in comparison to observations, which explains the large variability of simulated ozone at 200 hPa in West Europe and high northern latitudes between the different models.

For the evaluation of stratospheric processes including the UTLS, Eyring et al. (2010) have established the Chemistry-Climate Model Validation (CCMVal2) activity for coupled chemistry-climate models. We use the 10-day instantaneous model results between 1995 and 2004. The instantaneous model output allows us to calculate the

ACPD
11, 28747–28796, 2011

thermal TP and to consider tropopause-referenced altitudes. In addition, we derive the Hellinger distance between the CCMVal2 model results and observations. In Fig. 12 (first to third rows), we compare model results and observations at three pressure levels that are located in the UTLS and the stratosphere for the northern mid-latitudes. In addition, we evaluate tropopause-referenced altitudes (Fig. 12, fourth and fifth row). For seasonal comparisons, we derive monthly averages for each available year between 1995 and 2004 and then average over the entire period.

The seasonality of ozone is well captured by the models. Most regions and altitudes show a correlation coefficient > 0.9. Ozone is overestimated for all regions at 100 hPa and 50 hPa. This is because the TP for most models is shifted upwards by one or two levels (Eyring et al., 2010), as seems to be also the case for the HTAP models. Considering tropopause-referenced altitudes, ozone is overestimated above the TP (Fig. 12), especially in spring over the US and Japan, and in austral summer in the the SH mid-latitudes and polar region (not shown). The overestimation of ozone might be related to shortcomings of the representation of the stratospheric transport in the models in mid and high latitudes, consistent with Hegglin et al. (2010). In the SH, ozone is likely underestimated due to the underestimation of the ozone hole (see also Eyring et al. (2010), for a detailed evaluation of CCMVal2 model results). Mean differences between models and observations are discussed below.

The comparison of the Hellinger distance versus the median differences between models and the climatology for different regions (as introduced in Appendix B) allows some additional remarks on the representation of models, which go beyond the comparison of median differences alone. In general, we expect that the Hellinger distance and the median differences between models and observations are correlated. This is often the case, as shown as an example for West Europe for the lowermost stratosphere (Fig. 13). For West Europe, ozone medians and half-width of the distribution of CCMVal2 model results show a reasonable agreement between models and observations within the variability of the observations (Fig. 12, fourth and fifth row). Comparing the PDF and the Hellinger distance between models and observations (shown only for

ACPD
11, 28747–28796, 2011

one region as an example) indicates large shortcomings in the performance of different models with regard to the shape of the distribution (see Fig. 13, top row).

Especially in the upper troposphere, models perform very differently and show a large variability in the Hellinger distance and the median differences. For most models the Hellinger distance is much larger than the regional variability derived from observations (Fig. 13, small black points). In the lowermost stratosphere, the variability of the model performance is less compared to values within ±3 km around the TP. Various models reproduce the median value and the shape of the distribution reasonably well. However, there is still a high bias of ozone in many models compared to observations. Using the Hellinger distance as a diagnostic, we identify one model in 3–5 km above the TP (Fig. 13, right row, red line and symbols) that is not able to reproduce the shape of the distribution, even though the median of the distribution agrees with observations within 10 %.

For all regions in the lowermost stratosphere, the Hellinger distance for all considered models is much larger than the estimated range of the variability from observations of about 0.2, as illustrated in Fig. 14. The Hellinger distance is especially larger for those models that do not reproduce the median of the distribution, as expected. However, there are also models that reproduce the observed median of the ozone distribution reasonably well, but not the shape of the simulated distribution compared to the observed one. The median difference between models and observations reaches up to 150 %, the maximum Hellinger distance reached is 0.8. In summary, many models overestimate ozone in the lowermost stratosphere, whereas some regions are reproduced fairly well by a few models in the NH and to a lesser part in the SH, whereas all the models fail to reproduce ozone in the Tropics at 3–5 km above the TP.

8 Conclusions

A global ozonesonde climatology has been compiled using 41 stations. Monthly averaged ozone profiles between 1980–1994 and 1995–2009 are provided on pressure

ACPD
11, 28747–28796, 2011

altitudes and tropopause-referenced altitudes for all stations. For 1995–2009, sufficient observations are available to investigate the time evolution of ozone. The new ozone climatology between 1980–1994 agrees well with the climatology compiled by Logan (1999a,b). Between 1995–2009, ozone changes are smaller than observed for the earlier periods (e.g. Oltmans et al., 2010), however, some significant changes over the last 20 years can be identified. For example, we found a significant increase of tropospheric ozone (5–10 %) in high northern latitudes and a significant decrease of tropospheric ozone over West Europe and in Japan (in spring and summer), which supports the need for an updated ozone climatology, as provided here. It is important to note that changes in ozone between 1990–1999 and 2000–2009 vary with season, region and altitude, calling for caution while investigating deseasonalized ozone trends or averages over fixed altitude intervals.

Further, we aggregate stations with similar ozone characteristics into 9 regions to provide a robust data set for model evaluation. To quantify the variability of ozone within the defined regions, we calculate the Hellinger distance that compares the shape of two ozone distributions in addition to the median difference of two distributions. For high latitudes and West Europe in the UTLS, the Hellinger distance for different stations within one region is mostly below 0.15. This indicates a high degree of similarity between different stations within those regions. High variability in ozone distributions between different stations within one region occurs for the US and Japan in winter and spring in the lowermost stratosphere, with deviations of up to ±30 % from the regional mean and a Hellinger distance above 0.2. Ozone distributions for stations in the Tropics show a large variability below the tropopause, but are more similar above the tropopause with deviations from the regional median up to ± 20 % and a Hellinger distance of less than 0.1 for most of the stations.

The representativeness of regional aggregates is investigated by comparing ozone soundings with independent data sets, using surface ozone and MOZAIC aircraft data. Ozone soundings show excellent agreement (in both shape and median values) with these data sets for regions with a large number of observations, as is the case for

ACPD
11, 28747–28796, 2011

West Europe. This is not the case for other regions, like the US, since we only have 3 ozonesonde stations over a large area where significant differences exist for surface values. However, for most of the regions, especially in the free troposphere, the climatology agrees with surface and aircraft observations and therefore represents those regions reasonably well.

The seasonal variability of ozone profiles in the troposphere is in agreement with earlier studies (e.g., Logan, 1999a; McPeters et al., 2007). We further find longitudinal variations for different latitudes. For example, the western and eastern part of the NH polar region show different characteristics. This is also the case for the three regions in the NH mid-latitudes (West Europe, Japan and the US). Furthermore, the US and Japan show a different seasonality of ozone in the lowermost stratosphere than Europe, when considering tropopause-referenced altitudes. This may be related to a weaker transport barrier between the tropical TP and the lower stratosphere in the area around the Pacific in the NH in winter and spring (Wernli and Sprenger, 2007; Sprenger et al., 2007) and suggests a need for further investigation. The consideration of different regions in NH mid-latitudes and thereby longitudinal variations of ozone is important for the evaluation of models and has not been done to date.

The climatology is applied to evaluate model results from two different model intercomparison initiatives, HTAP, with focus on processes in the NH troposphere, and, CCMVal2, concentrating on the lower stratosphere and the UTLS. Simulated ozone profiles are interpolated to the ozonesonde sites considered in each region and regionally-aggregated ozone distributions are derived. This approach is recommended for model evaluations, because it leads to a valid comparison to the regionally-aggregated ozone frequency distribution from observations. A model comparison using regional averages can result in misleading results.

The models are in general able to reproduce the seasonality of ozone in the troposphere and stratosphere; however, discrepancies exist, especially in the UTLS. Differences in the height of the tropopause introduce differences between models and observations if considering pressure altitudes. Tropopause-referenced altitudes indicate

ACPD
11, 28747–28796, 2011

regional shortcomings of the models, e.g., an overestimation of ozone in the lowermost stratosphere especially in spring for the US and Japan, as well as in the SH austral summer. In general, ozone is overestimated in the lower stratosphere compared to observations, in agreement with Eyring et al. (2010). Further, the shape of ozone distributions in models is often very different from observed values. Implications of these shortcomings for the radiative forcing in the models have still to be investigated. In summary, the compiled ozonesonde climatology provides an updated and extended basis for present-day model evaluation that gives further insights on the ability of models to reproduce observed features of the global ozone distribution.

Appendix A

Data availability

The climatology is available at http://acd.ucar.edu/~tilmes/ozone.html. For each station and region we provide monthly averaged ozone profiles between 1000 and 10 hpa (in partial pressure and mixing ratios) for all available years between 1995 and 2009, as well as for the years between 1980 and 1994. Besides averaged profiles (mean and median), we provide information about the standard deviation, the half-width of the distribution (calculated as (75th percentile – 25th percentile)/2), and the number of profiles entering the average. Due to the lack of data from many stations in 1980 – 1994 we do not provide regional averages for the two periods considered. We further provide ozone profiles in tropopause-referenced altitude coordinates for the period between 1995 and 2009 for each station and region. For this, we calculated the thermal tropopause height (World Meteorological Organization, 1957) using temperature information from each sounding profile.

In addition, we provide seasonal averaged ozone timelines between 1995 and 2009, seasons are DJF, MAM, JJA, SON. We provide ozone median information for each year, the half-width of the distribution, and the number of profiles entering the

ACPD
11, 28747–28796, 2011

distribution for 26 pressure levels between 1000 hPa and 10 hPa. Furthermore, we provide the inter-annual variability, defined here as the range of the 5th and 95th percentile of annual median ozone values between 1995 and 2009 for all the pressure levels.

Appendix B

Hellinger distance

For the comparison of ozone distributions within observational data sets or between observations and models, the mean (or median) and standard deviation (or width) of a distribution are often considered, as discussed in Sect. 6. The comparison of means of ozone distributions does not give any information about the shape of the distributions, whereas the median and percentile give only a first-order estimate. However, a distribution of ozone concentrations is often not well represented as a Gaussian distribution, as shown in Fig. 15 (top row), using the ozone distribution based on sondes in Japan in LMS, as an example. Differences in the shape of two ozone distributions, e.g., Gaussian compared to bi-modal in the UTLS, even if describing the same mean and width of the distribution, might produce significantly different signals in radiative forcing or heating in a climate model. This is because the transmission of radiance along a path is exponential in the amount of material along a path. Thus, we would not expect the radiative forcing of the mean concentration to be the same as the mean of the distribution of radiative forcing from all samples, i.e., the mean of the function does not equal the function of the mean. Further, in the troposphere, the mean or median of a distribution does not give any information of the frequency of very high ozone episodes as a result of pollution that can lead to health problems. Consequently, we need to evaluate not only the differences between means of two distributions, but also how much the shape of the distributions vary from each other, to get an idea of how well the models represent the physical behavior of the atmosphere.

ACPD
11, 28747–28796, 2011

We introduce the "Hellinger distance" (Nikulin, 2001) as a tool to assess the similarity between two distributions. Let P and Q denote two probability measures that are absolutely continuous with respect to the ozone mixing ratio λ. The Hellinger distance $H(P,Q)$ between two cumulative distribution functions (CDF), P and Q of ozone, is defined as follows:

$$H^2(P,Q) = \frac{1}{2}\int\left(\sqrt{\frac{dP}{d\lambda}} - \sqrt{\frac{dQ}{d\lambda}}\right)^2 d\lambda \quad \text{(B1)}$$

$$0 \le H(p,q) \le 1 \quad \text{(B2)}$$

where dλ is the interval width of the mixing ratio bin. The Hellinger distance is 0 when two distributions are identical, and 1 when two distributions are completely different. The interval bin of the CDF is chosen in such a way that each bin contains an equal number of data, resulting in variable bin sizes. This allows a smoother representation of the shape of the CDF, as illustrated in Fig. 15, middle panel. To compare two distributions, the same number of bins and bin sizes are chosen for each distribution. Depending on the number of bins, the Hellinger distance can vary, however it does not change the conclusions. Here, we use 25 bins to compare two ozone distributions.

To illustrate the performance of Hellinger distance, we use the example of ozone distributions in the lowermost stratosphere (3–5 km above the tropopause) from the three Japanese data sets. Fig. 15, illustrates the PDF (top row) and CDF (middle row) of the ozone distributions taken from three different ozone sonde stations (different colors) for all four seasons. The three distributions are compared to the regional average (Fig. 15, middle row, black line), in calculating the Hellinger distance between the distribution of each station and the regionally-aggregated distribution. The derived Hellinger distance is then plotted against the percentage difference of the medians of the distributions, Fig. 15 (bottom row). In case the ozone distribution is very similar to the regional mean (black line), the Hellinger distance is below 0.1, as is the case in summer for all Japanese stations. On the other hand, even if the differences in the mean are small, the Hellinger distance can be larger than 0.2 if the shape of the three

ACPD
11, 28747–28796, 2011

ozone distributions is different, as is the case for winter and spring. In this example, airmasses for each of the three stations are rather similar and the Hellinger distance does not reach values above 0.3, as is also the case for most other regions considered (see Sect. 3). In contrast, the Hellinger distance can reach much larger values for comparisons between models and observations (see Sect. 7).

Supplementary material related to this article is available online at: http://www.atmos-chem-phys-discuss.net/11/28747/2011/acpd-11-28747-2011-supplement.pdf.

Acknowledgements. We gratefully acknowledge the effort of the The World Ozone and Ultraviolet Radiation Data Centre (WOUDC) and NOAA Earth system Research Laboratory (ESRL) for providing a collection of high quality ozone soundings. Further, we acknowledge the World Data Center for Greenhouse Gases (WDCGG), the Clean Air Status and Trends Network (CASTNET) and EMEP network for providing a collection of hourly surface observations. We further acknowledge the strong support of the European Commission, Airbus, and the Airlines (Lufthansa, Austrian, Air France) who carry free of charge the MOZAIC equipment and perform the maintenance since 5 1994. MOZAIC is presently funded by INSU-CNRS (France), Météo-France, and Forschungszentrum (FZJ, Jülich, Germany). The MOZAIC data based is supported by ETHER (CNES and INSU-CNRS). The HTAP and CCMVal2 modeling teams are acknowledged for sharing their results and Forschungszentrum Jülich and British Atmospheric Data Center (BADC) receive credit for hosting the HTAP and CCMVal2 data bases, respectively. We also thank Jennifer Wei for the helpful discussion on the use of correction factors. Andrew Conley was funded by the Department of Energy under the SciDAC program. The National Center for Atmospheric Research is funded by the National Science Foundation.

References

Birner, T. and Bönisch, H.: Residual circulation trajectories and transit times into the extratropical lowermost stratosphere, Atmos. Chem. Phys., 11, 817–827, doi:10.5194/acp-11-817-2011, 2011. 28763

ACPD
11, 28747–28796, 2011

Bönisch, H., Engel, A., Curtius, J., Birner, Th., and Hoor, P.: Quantifying transport into the lowermost stratosphere using simultaneous in-situ measurements of SF6 and CO_2, Atmos. Chem. Phys., 9, 5905–5919, doi:10.5194/acp-9-5905-2009, 2009. 28763

Bönisch, H., Engel, A., Birner, Th., Hoor, P., Tarasick, D. W., and Ray, E. A.: On the structural changes in the Brewer-Dobson circulation after 2000, Atmos. Chem. Phys., 11, 3937–3948, doi:10.5194/acp-11-3937-2011, 2011. 28762

Clain, G., Baray, J. L., Delmas, R., Diab, R., Leclair de Bellevue, J., Keckhut, P., Posny, F., Metzger, J. M., and Cammas, J. P.: Tropospheric ozone climatology at two Southern Hemisphere tropical/subtropical sites, (Reunion Island and Irene, South Africa) from ozonesondes, LIDAR, and in situ aircraft measurements, Atmos. Chem. Phys., 9, 1723–1734, doi:10.5194/acp-9-1723-2009, 2009. 28751

Crutzen, P. J.: A discussion of the chemistry of some minor constituents in the stratosphere and troposphere, Pure Appl. Geophys., 106–108, 1385–1399, 1973. 28749

Ding, A. J., Wang, T., Thouret, V., Cammas, J.-P., and Nédélec, P.: Tropospheric ozone climatology over Beijing: analysis of aircraft data from the MOZAIC program, Atmos. Chem. Phys., 8, 1–13, doi:10.5194/acp-8-1-2008, 2008. 28759

Emmons, L. K., Walters, S., Hess, P. G., Lamarque, J.-F., Pfister, G. G., Fillmore, D., Granier, C., Guenther, A., Kinnison, D., Laepple, T., Orlando, J., Tie, X., Tyndall, G., Wiedinmyer, C., Baughcum, S. L., and Kloster, S.: Description and evaluation of the Model for Ozone and Related chemical Tracers, version 4 (MOZART-4), Geosci. Model Dev., 3, 43–67, doi:10.5194/gmd-3-43-2010, 2010. 28754

Eyring, V., Shepherd, T. G., and Waugh, D. W.: SPARC Report on the Evaluation of Chemistry-Climate Models, SPARC Report No. 5, WCRP-132, WMO/TD-No.1526, 2010. 28750, 28763, 28766, 28767, 28771

Fiore, A. M., West, J. J., Horowitz, L. W., Naik, V., and Schwarzkopf, M. D.: Characterizing the tropospheric ozone response to methane emission controls and the benefits to climate and air quality., J. Geophys. Res., 113, D08307, doi:10.1029/2007JD009162, 2008. 28749, 28750, 28757, 28766

Folkins, I., Bernath, P., Boone, C., Lesins, G., Livesey, N., Thompson, A. M., Walter, K., and Witte, J. C.: Seasonal cycles of O_3, CO, and convective outflow at the tropical tropopause, Geophys. Res. Lett., 33, doi:10.1029/2006GL026602, 2006. 28764

Forster, P., Ramaswamy, V., Artaxo, P., Berntsen, T., Betts, R., Fahey, D., Haywood, J., Lean, J., Lowe, D., Myhre, G., Nganga, J., Prinn, R., Raga, G., Schulz, M., and Dorland, R. V.:

ACPD
11, 28747–28796, 2011

Changes in Atmospheric Constituents and in Radiative Forcing, in: Climate Change 2007: The Physical Science Basis. Contribution of Working Group I to the Fourth Assessment Report of the Intergovernmental Panel on Climate Change, Cambridge University Press, Cambridge, UK and New York, NY, USA, edited by: Solomon, S., Qin, D., Manning, M., Marquis, M., and Averyt, K., Tignor, M. B., Miller, H. L., and Chen, Z., 2007. 28749

Garcia, R. R. and Randel, W. J.: Acceleration of brewer-dobson circulation due to increase in greenhouse gases, J. Atmos. Sci., 65, 2731–2739, 2008. 28749

Gauss, M., Myhre, G., Isaksen, I. S. A., Grewe, V., Pitari, G., Wild, O., Collins, W. J., Dentener, F. J., Ellingsen, K., Gohar, L. K., Hauglustaine, D. A., Iachetti, D., Lamarque, F., Mancini, E., Mickley, L. J., Prather, M. J., Pyle, J. A., Sanderson, M. G., Shine, K. P., Stevenson, D. S., Sudo, K., Szopa, S., and Zeng, G.: Radiative forcing since preindustrial times due to ozone change in the troposphere and the lower stratosphere, Atmos. Chem. Phys., 6, 575–599, doi:10.5194/acp-6-575-2006, 2006. 28750

Hegglin, M. I., Gettelman, A., Hoor, P., Krichevsky, R., Manney, G. L., Pan, L. L., Son, S. W., Stiller, G., Tilmes, S., Walker, K. A., Eyring, V., Shepherd, T. G., Waugh, D., Akiyoshi, H., Añel, J. A., Austin, J., Baumgaertner, A., Bekki, S., Braesicke, P., Brühl, C., Butchart, N., Chipperfield, M., Dameris, M., Dhomse, S., Frith, S., Garny, H., Hardiman, S. C., Jöckel, P., Kinnison, D., Lamarque, J.-F., Mancini, E., Michou, M., Morgenstern, O., Nakamura, T., Olivié, D., Pawson, S., Pitari, G., Plummer, D. A., Pyle, J. A., Rozanov, E., Scinocca, J. F., Shibata, K., Smale, D., Teyssèdre, H., Tian, W., and Yamashita, Y.: Multimodel assessment of the upper troposphere and lower stratosphere: Extratropics, J. Geophys. Res., 115, D00M09, doi:10.1029/2010JD013884, 2010. 28767

Hess, P. G. and Zbinden, R.: Stratospheric impact on tropospheric ozone variability and trends: 1990–2009, Atmos. Chem. Phys. Discuss., 11, 22719–22770, doi:10.5194/acpd-11-22719-2011, 2011. 28760

Keating, T. J. and Zuber, A.: Task Force on Hemispheric Transport of Air Pollution, Air Pollut. Stud. 16, U.N. Econ. Comm. for Europe, New York, hemispheric transport of air pollution 2007 interim report, 2007. 28766

Kunz, A., Pan, L. L., Konopka, P., Kinnison, D., and Tilmes, S., Chemical and dynamical discontinuity at the extratropical tropopause based on start08 and waccm analyses, J. Geophys. Res., accepted, 2011. 28749

Lamarque, J.-F., Hess, P., Emmons, L., Buja, L., Washington, W., and Granier, C.: Tropospheric ozone evolution between 1890 and 1990, J. Geophys. Res., 110, D08304,

ACPD
11, 28747–28796, 2011

doi:10.1029/2004JD005537, 2005. 28750
Lefohn, A., Oltmans, S., Dann, T., and Singh, H.: Presentday variability of background ozone in the lower troposphere, J. Geophys. Res., 106, 9945–9958, 2001. 28764
Lelieveld, J. and Dentener, F. J.: What controls the tropospheric ozone, J. Geophys. Res., 105, 3543–3563, 2000. 28749
Logan, J. A.: An analysis of ozonesonde data for the troposphere: Recommendations for testing 3-D models and development of a gridded climatology for tropospheric ozone, J. Geophys. Res., 104, 16115–16150, 1999a. 28751, 28754, 28761, 28763, 28769, 28770
Logan, J. A.: An analysis of ozonesonde data for the lower stratosphere: Recommendations for testing models, J. Geophys. Res., 104, 16151–16170, 1999b. 28751, 28769
McPeters, R. D., Labow, G. J., and Logan, J. A., Ozone climatological profiles for satellite retrieval algorithms, Geophys. Res. Lett., 112, D05308, doi:10.1029/2005JD006823, 2007. 28751, 28770
Nikulin, M. S.: Hellinger distance, in Encyclopeadia of Mathematics, edited by: M. Hazewinkel, Springer, 2001. 28751, 28773
Oltmans, S., Lefohn, A., Harris, J. M., Galbally, I., Scheel, H., Bodeker, G., Brunke, E., Claude, H., Tarasick, D., Johnson, B., Simmonds, P., Shadwick, D., Anlauf, K., Hayden, K., Schmidlin, F., Fujimoto, T., Akagi, K., Meyer, C., Nichol, S., Davies, J., Redondas, A., and Cuevas, E.: Long-term changes in tropospheric ozone, Atmos. Environ., 40, 3156–3173, 2006. 28751, 28761
Oltmans, S. J., Lefohn, A. S., Harris, J. M., Tarasick, D. W., Thompson, A. M., Wernli, H., Johnson, B. J., Novelli, P. C., Montzka, S. A., Ray, J. D., Patrick, L. C., Sweeney, C., Jefferson, A., Dann, T., Davies, J., Shapiro, M., and Holben, B. N.: Enhanced ozone over western north america from biomass burning in eurasia during april 2008 as seen in surface and profile observations, Atmos. Environ., 44, 4497–4509, 2010. 28749, 28769
Pan, L. L., Randel, W. J., Gary, B. L., Mahoney, M. J., and Hintsa, E. J., Definitions and sharpness of the extratropical tropopause: A trace gas perspective, J. Geophys. Res., 109, doi:10.1029/2004JD004982, 2004. 28765
Pan, L. L., Bowman, K. P., Atlas, E. L., Wofsy, S. C., Zhang, F., Bresch, J. F., Ridley, B. A., Pittman, J. V., Homeyer, C. R., Romashkin, P., and Cooper, W. A.: The StratosphereTroposphere Analyses of Regional Transport 2008 experiment, B. Am. Meteorol. Soc., 91, 327–342, 2010. 28751
Randel, W. and Thompson, A.: Interannual variability and trends in tropical ozone derived from

ACPD
11, 28747–28796, 2011

SAGE II satellite data and SHADOZ ozonesondes, J. Geophys. Res., in press, 2011. 28751, 28760, 28765
Randel, W. J., Park, M., and Wu, F.: A large annual cycle in ozone above the tropical tropopause linked to the Brewer-Dobson circulation, J. Atmos. Sci., 64, 4479–4488, 2008. 28764
Reichler, T. and Kim, J.: How well do coupled models simulate todays climate?, B. Am. Meteorol. Soc., 89, 303–311, 2008. 28750
Reidmiller, D. R., Fiore, A. M., Jaffe, D. A., Bergmann, D., Cuvelier, C., Dentener, F. J., Duncan, B. N., Folberth, G., Gauss, M., Gong, S., Hess, P., Jonson, J. E., Keating, T., Lupu, A., Marmer, E., Park, R., Schultz, M. G., Shindell, D. T., Szopa, S., Vivanco, M. G., Wild, O., and Zuber, A.: The influence of foreign vs. North American emissions on surface ozone in the US, Atmos. Chem. Phys., 9, 5027–5042, doi:10.5194/acp-9-5027-2009, 2009. 28759
Rex, M., Salawitch, R. J., von der Gathen, P., Harris, N. R. P., Chipperfield, M. P., and Naujokat, B.: Arctic ozone loss and climate change, Geophys. Res. Lett., 31, doi:0.1029/2003GL018844, 2004. 28750
Smit, H. G. R., Sträter, W., Helten, M., Kley, D., Ciupa, D., Claude, H. J., Köhler, U., Hoegger, B., Levrat, G., Johnson, B., Oltmans, S. J., Kerr, J. B., Tarasick, C. W., Davies, J., Shitamichi, M., Srivastav, S. K., Vialle, C., and Velghe, G., JOSIE: The 1996 WMO international intercomparison of ozonesondes under quasi flight conditions in the environmental simulation chamber at Jülich, in Atmospheric Ozone, Proceedings of the Quadrennial Ozone Symposium 1996, L'Aquila, 971–974, 1998. 28751, 28753
Sprenger, M., Wernli, H., and Bourqui, M.: Stratospheretroposphere exchange and its relation to potential vorticity streamers and cutoffs near the extratropical tropopause, J. Atmos. Sci., 64, 1587–1602, 2007. 28749, 28764, 28770
Stevenson, D. S., Dentener, F. J., Schultz, M. G., et al.: Multi-model ensemble simulations of present-day and near-future tropospheric ozone, J. Geophys. Res., 111, D08301, doi:10.1029/2005JD006338, 2006. 28749, 28750
Tang, Q. and Prather, M. J.: Correlating tropospheric column ozone with tropopause folds: the Aura-OMI satellite data, Atmos. Chem. Phys., 10, 9681–9688, doi:10.5194/acp-10-9681-2010, 2010. 28749
Tarasick, D. W., Fioletov, V. E., Wardle, D. I., Kerr, J. B., and Davies, J.: Changes in the vertical distribution of ozone over Canada from ozonesondes: 1980–2001, J. Geophys. Res., 110, doi:10.1029/2004JD004643, 2005. 28760
Thompson, A. M., Allen, A. L., Lee, S., Miller, S. K., and Witte, J. C., Gravity and rossby

ACPD
11, 28747–28796, 2011

wave signatures in the tropical troposphere and lower stratosphere based on southern hemisphere additional ozonesondes (SHADOZ), 1998–2007, J. Geophys. Res., 116, D05302, doi:10.1029/2009JD013429, 2011a. 28751, 28763, 28765

Thompson, A. M., Oltmans, S. J., Tarasick, D. W., der Gathen, P. V., Smit, H. G. J., and Witte, J. C.: Strategic ozone sounding networks: Review of design and accomplishments, Atmos. Environ., 45, 2145–2163, 2011b. 28749, 28751, 28755, 28760, 28763, 28765

Thompson, A. M., Witte, J. C., McPeters, R. D., Oltmans, S. J., Schmidlin, F. J., Logan, J. A., Fujiwara, M., Kirchhoff, V. W. J. H., Posny, F., Coetzee, G. J. R., Hoegger, B., Kawakami, S., Ogawa, T., Johnson, B. J., Vömel, H., and Labow, G.:Southern Hemisphere Additional Ozonesondes (SHADOZ) 1998 – 2000 tropical ozone climatology 1. Comparison with Total Ozone Mapping Spectrometer (TOMS) and ground-based measurements, J. Geophys. Res., 108, 8238, 2003a. 28751, 28752

Thompson, A. M., Witte, J. C., Oltmans, S. J., Schmidlin, F. J., Logan, J. A., Fujiwara, M., Kirchhoff, V. W. J. H., Posny, F., Coetzee, G. J. R., Hoegger, B., Kawakami, S., Ogawa, T., Fortuin, J. P. F., and Kelder, H. M.: Southern Hemisphere Additional Ozonesondes (SHADOZ) 1998–2000 tropical ozone climatology 2. tropospheric variability and the zonal wave-one, J. Geophys. Res., 108, 8241, 2003b. 28752

Thompson, A. M., MacFarlane, A. M., Morris, G. A.; Yorks, J. E., Miller, S. K., Taubman, B. F., Verver, G.; Vömel, H., Avery, M. A.; Hair, J. W.; Diskin, G. S.; Browell, E. V., Canossa, J. V., Kucsera, T. L., Klich, C. A., and Hlavka, D. L.: Convective and wave signatures in ozone profiles over the equatorial Americas: Views from TC4 2007 and SHADOZ, J. Geophys. Res., 115, D00J23, doi:10.1029/2009JD012909, 2010. 28763

Thouret, V., Marenco, A., Logan, J., Ndlec, P., and Grouhel, C., Comparisons of ozone measurements from the MOZAIC airborne program and the ozone sounding network at eight locations, jgr, 1003, 25695–25720, 1998a. 28751

Thouret, V., Marenco, A., Nédélec, P., and Grouhel, C.: Ozone climatologies at 9–12 km altitude as seen by the MOZAIC airborne program between September 1994 and August 1996., J. Geophys. Res., 103, 1998b. 28752, 28757

Thouret, V., Cammas, J.-P., Sauvage, B., Athier, G., Zbinden, R., Nédélec, P., Simon, P., and Karcher, F.: Tropopause referenced ozone climatology and inter-annual variability (1994–2003) from the MOZAIC programme, Atmos. Chem. Phys., 6, 1033–1051, 2006, http://www.atmos-chem-phys.net/6/1033/2006/. 28763, 28764

Tilmes, S., Pan, L., Hoor, P., Sachse, G. W., Loewenstein, M., Lopez, J., Webster, C.,

ACPD
11, 28747–28796, 2011

Cristensen, L. E., Proffitt, M., Gao, R.-S., Diskin, G. S., Avery, M. A., Podolske, J. R., Herman, R. L., Spelten, N., Weinheimer, A., Campus, T., Hintsa, E. J., Weinstock, E. M., Pittman, J., Zondl, M. A., Paige, M. E., and Atlas, E.: An aircraft based upper troposphere lower stratosphere O_3, CO and H_2O climatology for the northern hemisphere, J. Geophys. Res., 115, D14303, doi:10.1029/2009JD012731, 2010. 28750, 28751, 28763, 28764

Vingarzan, R.: A review of surface ozone background levels and trends, Atmos. Environ., 38, 3431–3442, 2004. 28749

Wernli, H. and Sprenger, M.: Identification and ERA-15 climatology of potential vorticity streamers and cutoffs near the extratropical tropopause, J. Atmos. Sci., 64, 1569–1586, 2007. 28749, 28764, 28770

WMO: Scientific assessment of ozone depletion: 2006, Global Ozone Research and Monitoring Project-Report No. 50, Geneva, Switzerland, 2007. 28749

WMO:Scientific assessment of ozone depletion: 2010, Global Ozone Research and Monitoring Project-Report No. 51, Geneva, Switzerland, 2010. 28749

World Meteorological Organization: Meteorology – A three-dimensional science, WMO Bull 6, 1957. 28756, 28771, 28791

ACPD

11, 28747–28796, 2011

Table 1. Number ozone profiles per season and period considered, Period I: 1980–1994, Period II: 1995–2009.

Station	Period I	DJF	MAM	JJA	SON	Period II	DJF	MAM	JJA	SON
Alert	1987–1994	133	90	70	69	1995–2008	163	153	130	138
Eureka	1992–1994	22	17	16	22	1995–2008	354	281	157	156
NyAlesund	1990–1994	163	128	79	97	1995–2006	378	322	180	187
Resolute	1980–1994	120	145	139	127	1995–2007	125	102	90	92
Scoresbysund	1989–1994	42	50	51	51	1995–2003	139	110	93	98
Lerwick	1992–1994	31	7	8	10	1995–2008	263	202	138	161
Churchill	1980–1994	112	133	143	132	1995–2007	150	149	109	122
Edmonton	1980–1994	122	137	137	121	1995–2008	156	193	165	154
Goosebay	1980–1994	136	151	134	131	1995–2007	151	147	148	141
Legionowo	1993–1994	3	3	10	11	1995–2009	251	237	186	178
Lindenberg	1992–1994	38	24	27	21	1995–2009	198	188	196	169
Debilt	1992–1994					1995–2009	110	93	101	112
Uccle	1980–1994	278	356	359	342	1995–2007	414	446	496	449
Praha	1992–1994	44	68			1995–2009	320	490		
Hohenpeissenberg	1980–1994	499	456	353	393	1995–2009	484	461	377	411
Payerne	1980–1994	380	391	414	420	1995–2009	532	555	545	545
Sapporo	1980–1994	45	58	60	58	1995–2009	157	159	142	154
Madrid	1994–1994					1995–2009	131	131	134	126
Boulder	1993–1994	9	12	9	7	1995–2009	150	162	208	164
WallopsIsland	1980–1994	76	76	76	76	1995–2009	207	204	229	231
Tateno	1980–1994	116	99	93	102	1995–2009	221	220	157	166
Huntsville	1980–1994					1999–2007	114	155	166	131
Kagoshima	1980–1994	47	53	48	60	1995–2005	132	112	109	126
Naha	1989–1994	37	31	32	37	1995–2008	140	141	132	145
Hongkong	1980–1994					2000–2007	64	84	74	77
Paramaribo	1980–1994					1999–2008	81	86	91	99
Hilo	1980–1994					2007–2007	119	162	147	144
Sancristobal	1980–1994					1998–2008	82	90	108	122
Nairobi	1980–1994					1996–2009	119	140	139	142
Natal	1980–1994	18	29	44	38	1995–2009	103	110	110	109
Ascension	1990–1994	15	16	22	34	1995–2009	121	132	125	156
Watukosek	1980–1994					1998–2009	48	53	66	72
Samoa	1980–1994					1995–2009	115	120	118	121
Fiji	1980–1994					1997–2008	64	88	78	75
Reunion	1980–1994					1998–2009	73	95	87	89
Broadmeadows	1980–1994					1999–2009	56	75	79	78
Lauder	1986–1994	47	40	60	86	1995–2008	139	154	144	172
Macquarie	1994–1994					1995–2009	90	109	110	102
Marambio	1988–1994	27	31	44	95	1995–2009	49	35	108	124
Neumayer	1992–1994	16	18	25	42	1995–2009	215	182	242	361
Syowa	1980–1994	62	60	64	126	1995–2009	176	164	227	266

ACPD
11, 28747–28796, 2011

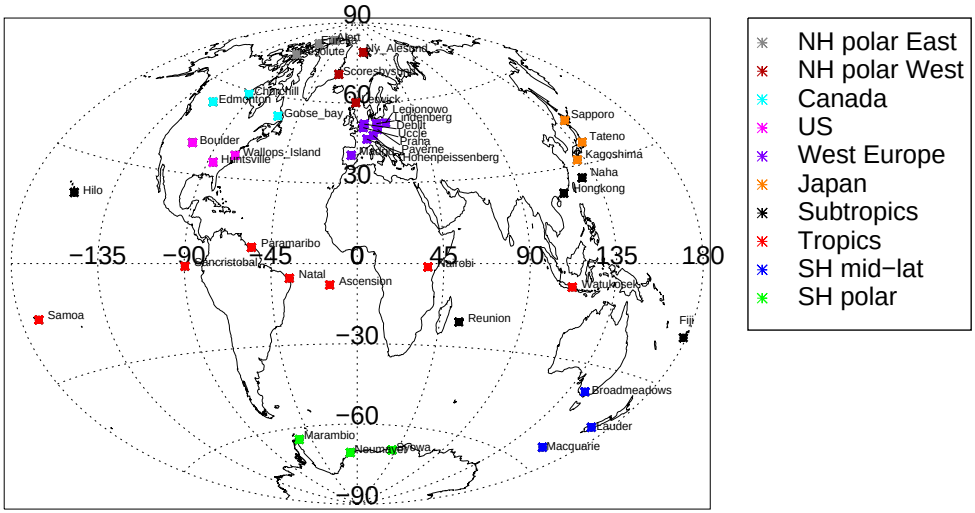

Fig. 1. Selected Ozone sondes, different colors denote different regions: NH Polar East: gray, NH Polar West: brown, Canada: cyan, United States of America (US): pink, West Europe: purple, Japan: orange, Subtropics: black, Tropics: red, SH Mid-latitudes: blue, SH Polar: green. Those stations that are not included in selected regions are shown in black.

ACPD
11, 28747–28796, 2011

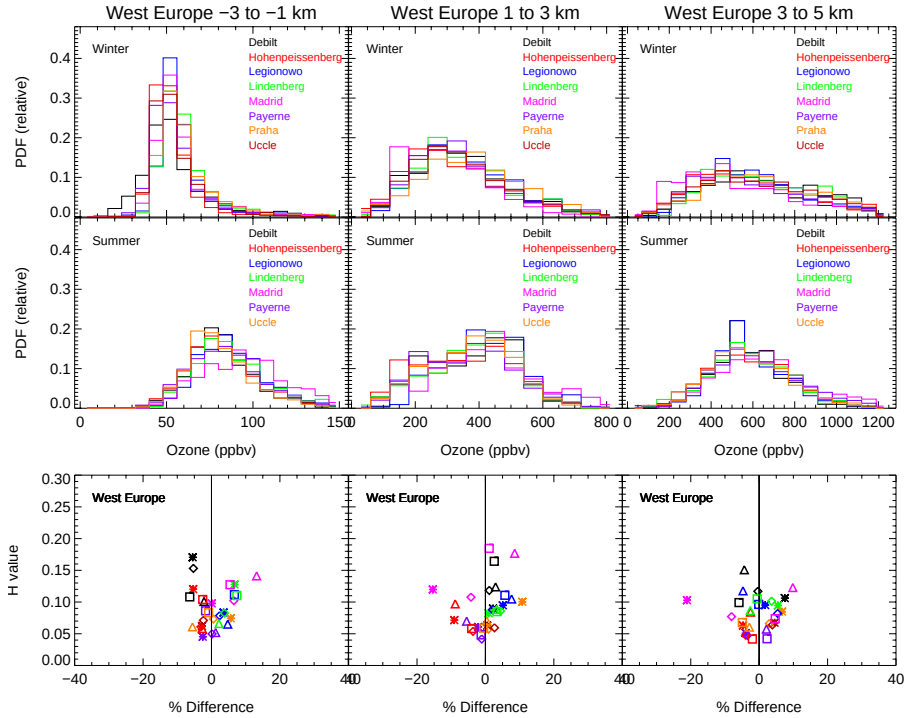

Fig. 2. Top and middle row: probability distribution function (PDF) of UTLS ozone for different stations within West Europe (different colors) for winter (top) and summer (middle) with regard to the thermal tropopause. Bottom panel: Hellinger Distance between the ozone distribution of single stations and the regionally-aggregated distribution versus the median differences of the two distributions, shown for all stations (different colors) and seasons (winter: asterisks, spring: diamonds, summer: triangles, fall: squares). Distribution samples are from the vertical regions 1–3 km below the tropopause (left), 1–3 km above the tropopause (middle) and in 3–5 km above the tropopause (right).

ACPD
11, 28747–28796, 2011

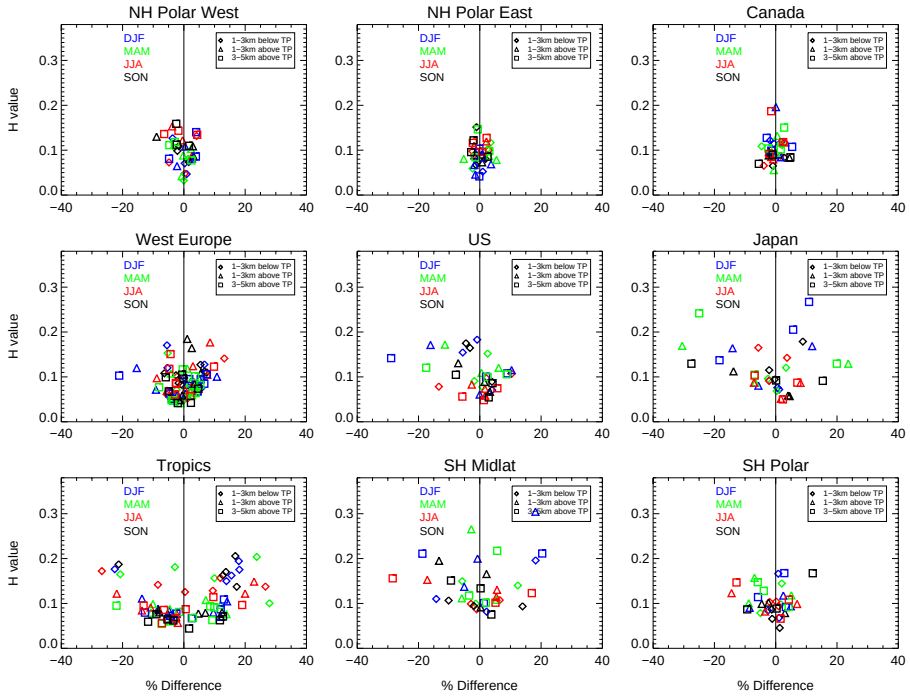

Fig. 3. Hellinger Distance for UTLS ozone at different stations with regard to the regionally-aggregated distribution, plotted against the difference of medians between the two distributions, shown for all seasons (different colors) and regions (different panels). Distribution samples are from the vertical regions 1–3 km below the TP (asterisks), 1–3 km above the TP (diamonds) and in 3–5 km above the TP (triangles).

ACPD
11, 28747–28796, 2011

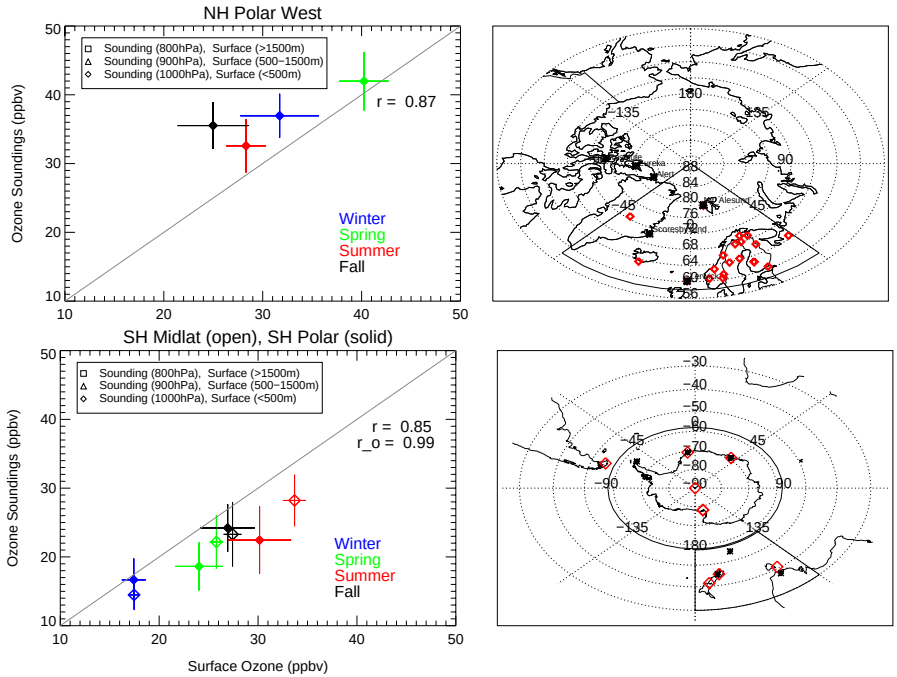

Fig. 4. Right panels: Location of ozone soundings (black stars) and surface observations (red diamonds) for two regions. Surface stations are taken from EMEP and WDCGG for the NH Polar region and from WDCGG for the SH. Left panels: Correlation between averaged ozone soundings and surface ozone observations for each region (as shown in the right panel) using available observations between 1995 and 2009. Error bars indicate the interannual variability of seasonal and regional aggregates for each region and altitude range between 1995 and 2009. For the SH (right bottom panel), filled symbols are correlations for SH Polar, whereas open symbols illustrate the correlation performed for soundings and surface data for SH mid-latitudes. Different colors are denoted to different seasons.

ACPD
11, 28747–28796, 2011

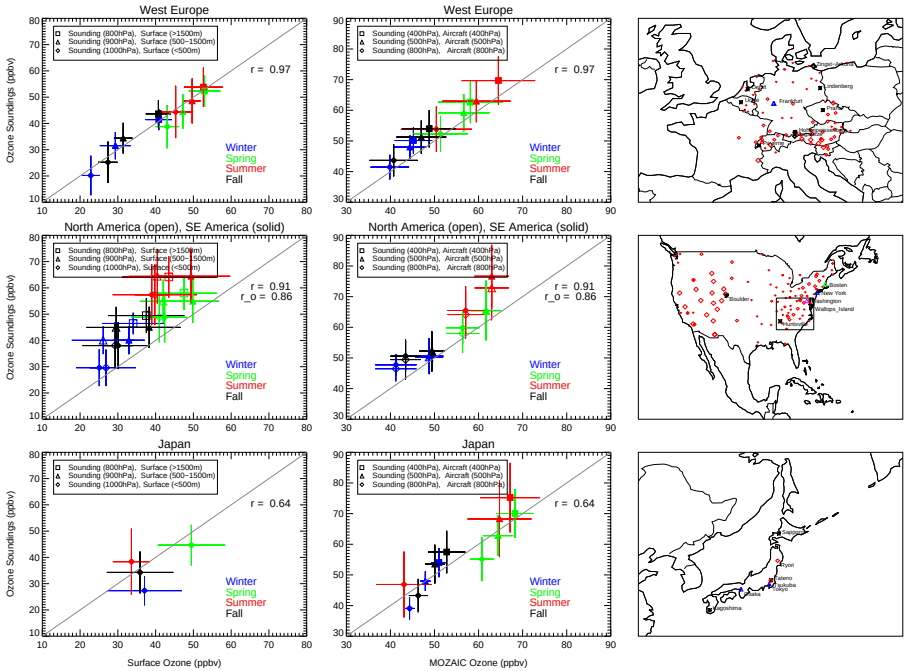

Fig. 5. Right panels: Location of ozone soundings (black stars), surface observations (red diamonds) and MOZAIC aircraft observations (blue triangles). Surface stations are taken from EMEP for West Europe, from CASTNET for the US, from WDCGG for Japan. Different symbol sizes indicate the altitude information of surface stations. Left panel: the same as Fig. 4 left panel, but for two different regions. For West Europe, hourly surface data are selected for the area around Frankfurt, Germany, and are averaged for a time between 10:00 and 14:00 UTC, in agreement to the time when ozone soundings are usually taken in this region. Middle panel: Correlation between averaged ozone soundings and MOZAIC aircraft observations for each region (as shown in the right panel) using available observations between 1995 and 2009.

ACPD
11, 28747–28796, 2011

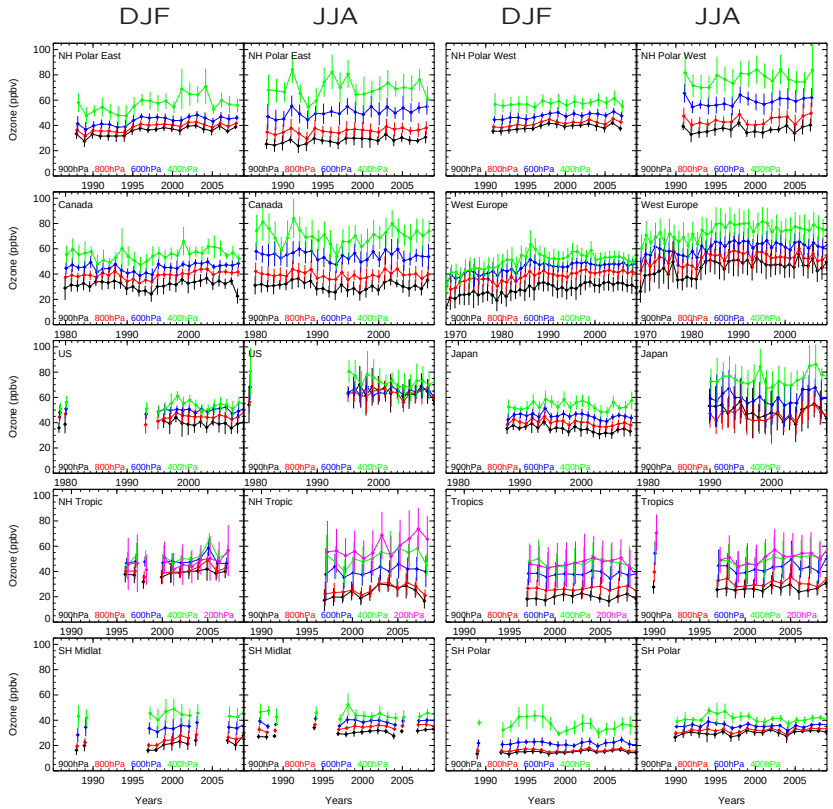

Fig. 6. Time evolution of from soundings for different pressure levels for different seasons (DJF and JJA) and regions. Different colors indicate different altitude levels. Symbols show the median; error bars show the half-width of the distribution (the range of the 25th and 75th percentile). The number of soundings entering each median value each season and year is at least 12. In addition to the regions shown in Fig. 1, the Northern Hemisphere Tropics region is included also.

ACPD
11, 28747–28796, 2011

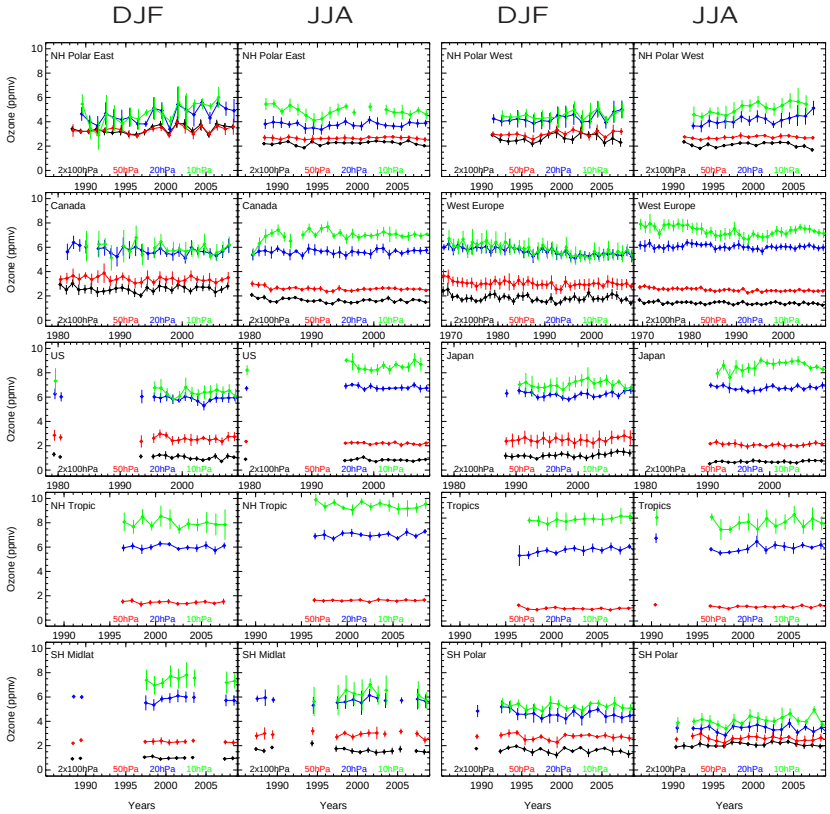

Fig. 7. As Fig. 6 but for additional pressure levels. Ozone values for the 100 hPa pressure levels are multiplied by a factor of two for illustrative reasons. For the same region, this level is not shown for the tropics.

ACPD
11, 28747–28796, 2011

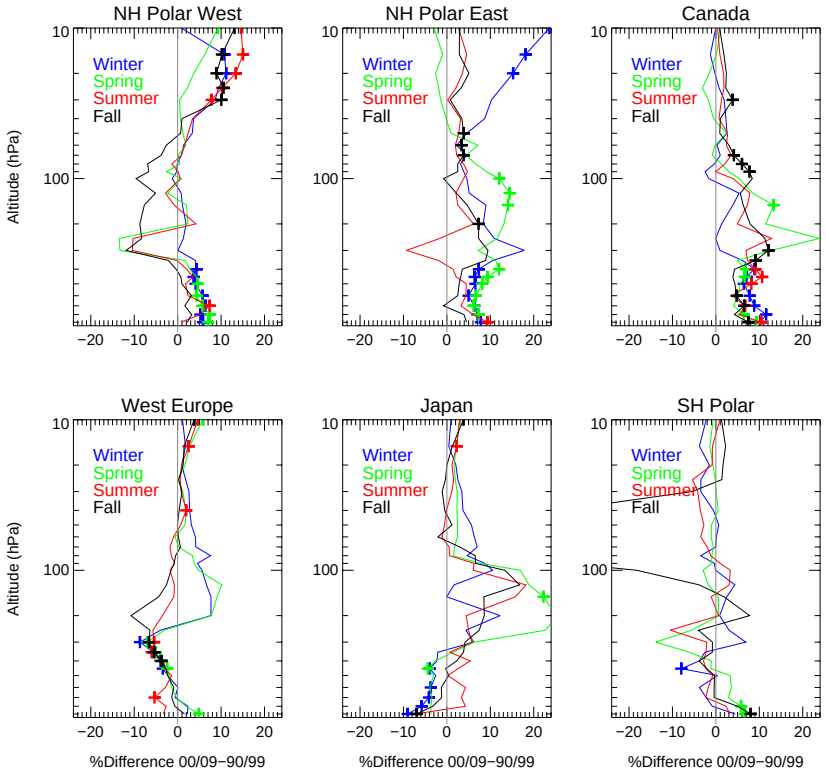

Fig. 8. Percent differences of annual median ozone mixing ratios between the periods 1990–1999 and 2000–2009. Different seasons are illustrated in different colors. Differences that are significant at the 95 % level based on the Student's t test are shown as plus signs. Minimum values in the SH polar region exceed −50 %.

ACPD
11, 28747–28796, 2011

Ozonesonde climatology between 1995 and 2009

S. Tilmes et al.

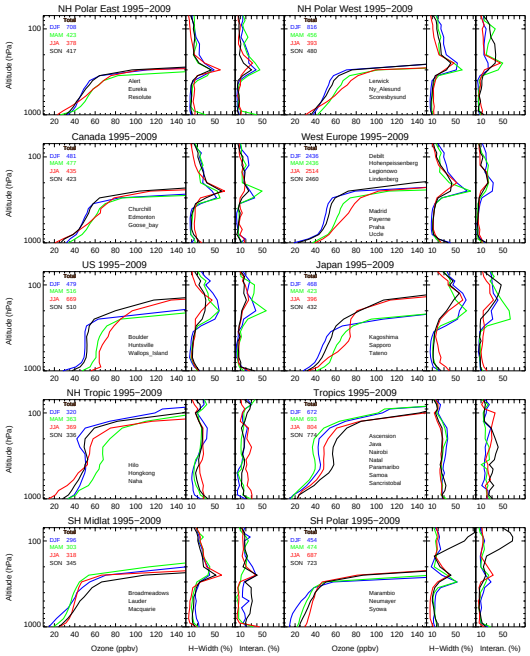

Fig. 9. Altitude distributions (median) of ozone soundings averaged for different seasons and regions between 1995 and 2009. Different colors indicate different seasons. The total number of profiles used for each season and region is shown on the top left of each panel. The stations entering the profiles are noted in the lower right of each panel. The half-width of the distribution (left) and the interannual variability (right) of each averaged profile are illustrated on two sub-plots on the right of each panel. The half-width of the distribution is defined here as the range of the 25th and 75th percentile of the annual ozone distribution (calculated as: (75th percentile – 25th percentile)/2.) averaged over all the years. The interannual variability is defined as the range of the 5th and 95th percentile of the annual median ozone value (calculated as: (95th percentile – 5th percentile)/2.) for all seasons and regions.

ACPD
11, 28747–28796, 2011

Ozonesonde climatology between 1995 and 2009

S. Tilmes et al.

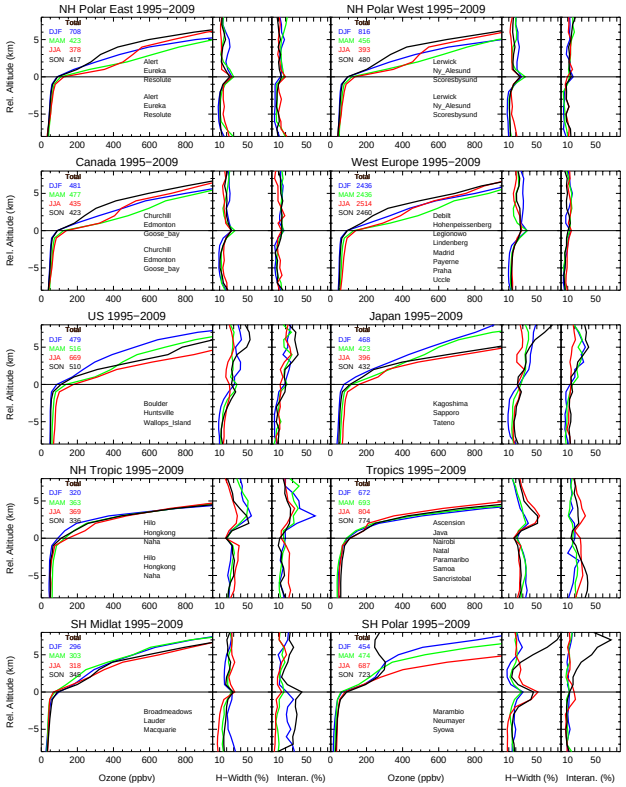

Fig. 10. As Fig. 9, but showing ozone profiles relative to the thermal tropopause (World Meteorological Organization, 1957).

ACPD
11, 28747–28796, 2011

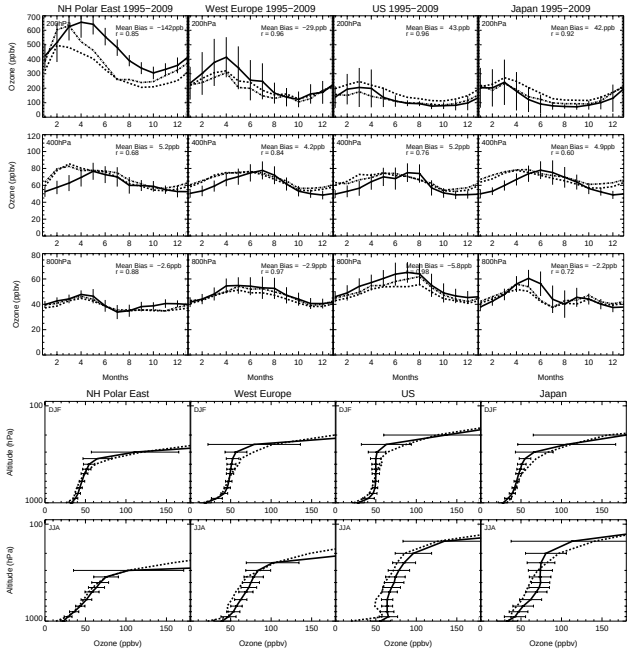

Fig. 11. First to third row: Comparison of the seasonality of ozone mixing ratios at three pressure levels and for four regions, one in high northern latitudes (left column) and three in the NH mid-latitudes between the ozone climatology and HTAP model results. Monthly averaged median values from the climatology are shown as solid black lines. The half-width of the distribution is shown as error bars. Monthly averaged model results for one available year (2001) were used to derive the multi-model mean and median (dashed and dashed-dotted lines, respectively). The bias between the model mean and the multi-model mean and the observational climatology is given at the right top corner of each panel, as well as the correlation coefficient between the two distributions. Fourth and fifth row: comparison of vertical ozone profiles for two seasons using ozone soundings and HTAP, corresponding to the regions of the first three rows.

ACPD
11, 28747–28796, 2011

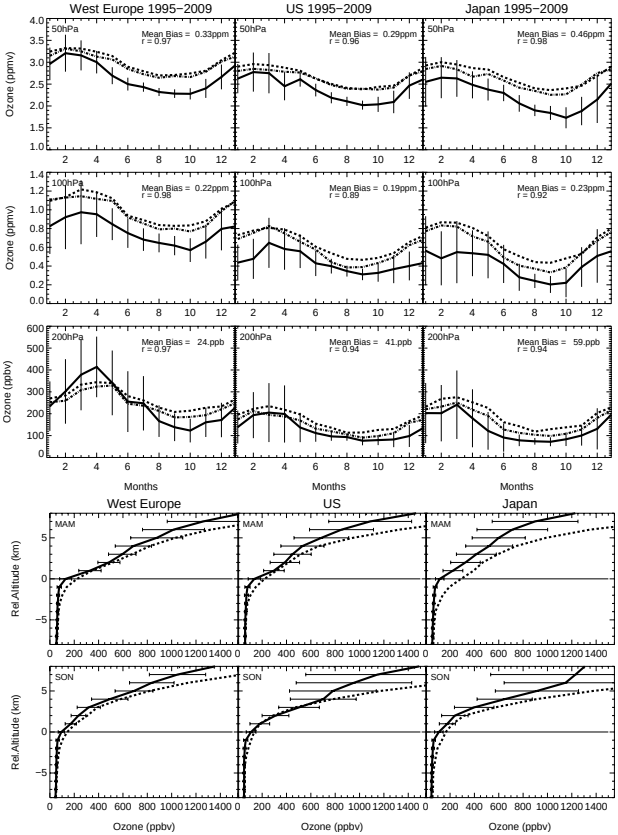

Fig. 12. Same as Fig. 11, but for different pressure levels and only three regions using CCM-Val2 model results. CCMVal2 monthly averages are calculated from 10 yr of 10-day instantaneous model output for each of the 15 models.

ACPD
11, 28747–28796, 2011

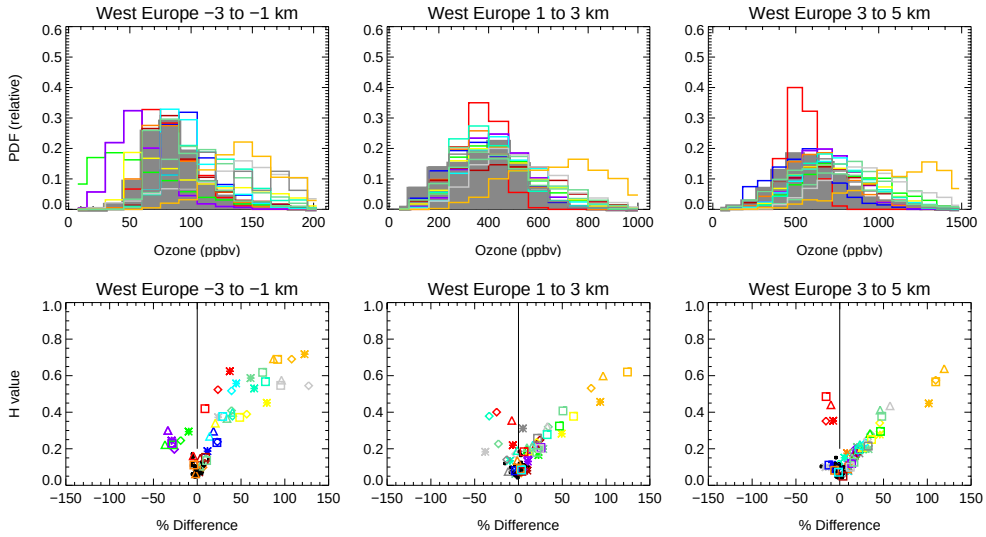

Fig. 13. Top row: probability distribution function (PDF) of the regionally-aggregated ozone distribution for West Europe (grey shaded area) in comparison to regionally-aggregated ozone distributions from model results (different colors), for summer only. Bottom panel: Hellinger distance between the climatological ozone distribution and each of the modeled distributions, as shown for summer in the top panel, is plotted against the relative difference of the medians of the two distributions. Different colors illustrate the Hellinger distance for different models, different symbols illustrate different seasons: winter (asterisk), spring (square), summer (triangle), and winter (diamond). Black small asterisks are values taken from Fig. 3, to illustrate the variability of Hellinger distances within one region, based on observations. Distribution samples are from the vertical regions 1–3 km below the TP (left), 1–3 km above the TP (middle) and in 3–5 km above the TP (right).

ACPD
11, 28747–28796, 2011

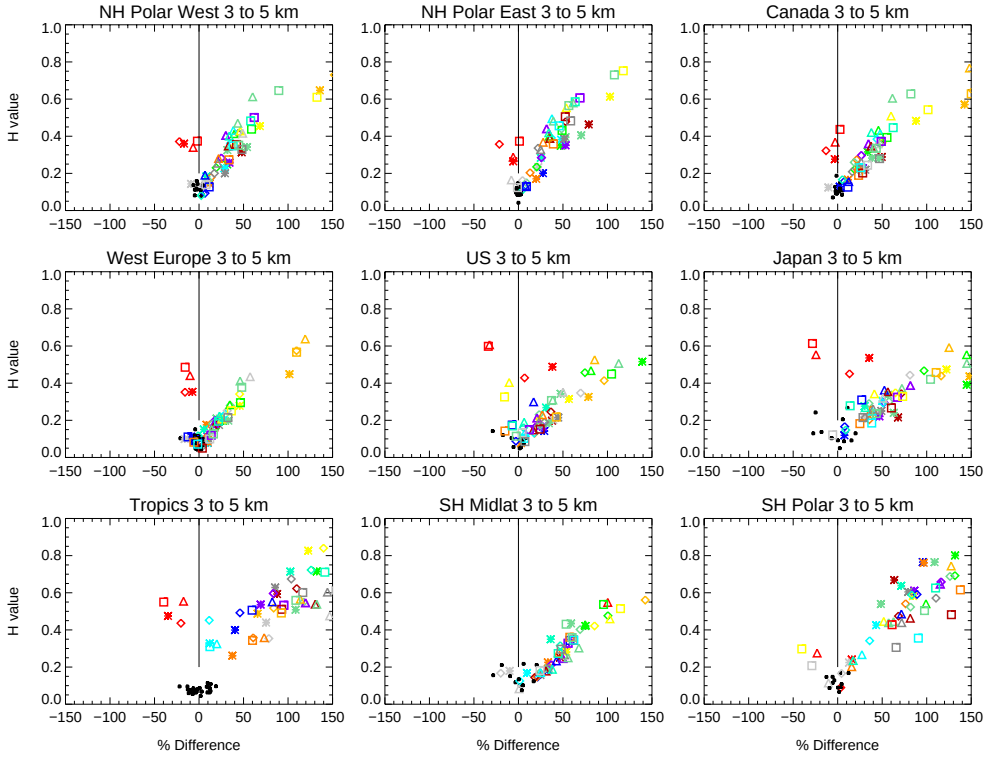

Fig. 14. As Fig. 13, but for all regions considered and for 3–5 km above the TP.

ACPD
11, 28747–28796, 2011

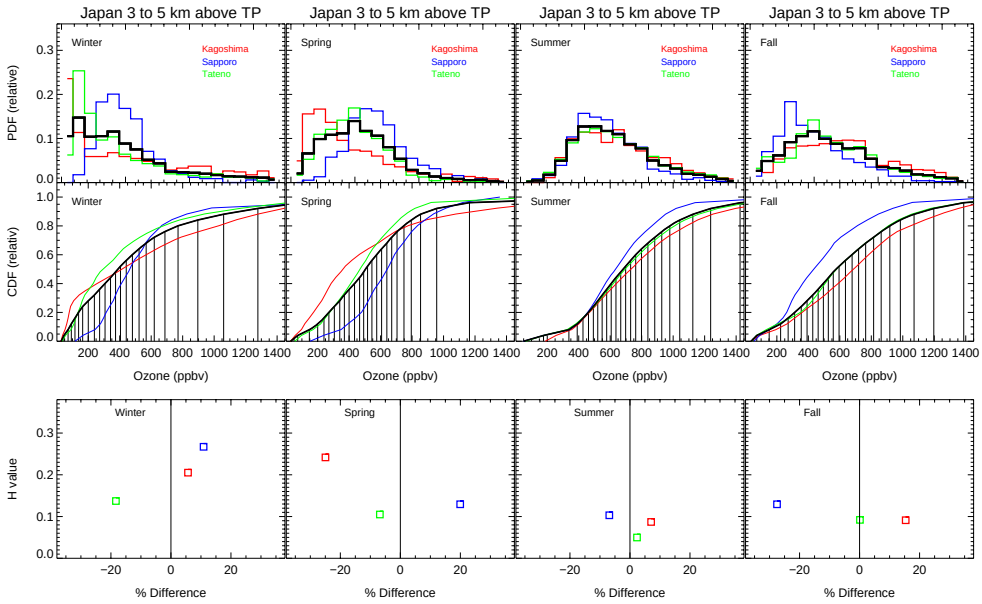

Fig. 15. Top row: probability distribution function (PDF) of ozone for the three stations within Japan (different colors) for four seasons. The regionally-aggregated distribution is shown as black thick lines. Middle row: Cumulative Distribution Functions (CDF) of ozone for the three stations (thin lines) and for the regionally-aggregated distribution (average distribution of ozone from all three stations (thick black line)) using variable bin sizes for the underlying PDF. Bottom panel: Hellinger distance between different stations (different colors) and the regionally-aggregated distribution plotted against the median differences of the two distributions. Distribution samples are from data within 3–5 km above the TP.

ACPD
11, 28747–28796, 2011